

CrossMark  
click for updatesCite this: *RSC Adv.*, 2016, 6, 52009

# Coordination chemistry of pyrazine derivatives analogues of PZA: design, synthesis, characterization and biological activity†

Małgorzata Ogryzek,<sup>a</sup> Agnieszka Chylewska,<sup>\*a</sup> Aleksandra Królicka,<sup>b</sup> Rafał Banasiuk,<sup>b</sup> Katarzyna Turecka,<sup>c</sup> Dorota Lesiak,<sup>d</sup> Dawid Nidzworski<sup>de</sup> and Mariusz Makowski<sup>\*a</sup>

Ru(III) complexes with pyrazine derivatives: 2,3-bis(2-pyridyl)pyrazine (*DPP*), pyrazine-2-amidoxime (*PAOX*), pyrazine-2-thiocarboxamide (*PTCA*) and 2-amino-5-bromo-3-(methylamino)pyrazine (*ABMAP*) have been prepared. Characterization of the compounds was acquired using UV-Vis and FT-IR spectroscopy, elemental analysis, conductivity and electrochemical measurements as well as thermogravimetric studies. The ligand field parameters,  $\Delta_0$  (splitting parameter),  $B$  (Racah parameter of interelectronic repulsion) and  $\beta$  (nephelauxetic ratio) were calculated. The stabilities of the Ru(III) complexes have also been confirmed by spectrophotometric titration methods in acetonitrile and water solutions. The data showed that the examined compounds are stable both in solution and solid states, which was also confirmed by the values of their stability constants found. Moreover, the molecular structures of the complexes have been optimized using AM1 and PM3 methods and this supported octahedral geometry around the Ru(III) ion. The minimum inhibitory (MIC) and minimum bactericidal concentration (MBC) for synthesized complexes were studied against two Gram (+) bacteria, two Gram (–) bacteria and fungi – three reference strains of *Candida albicans*. The results show that [RuCl(*PAOX*)<sub>2</sub>(OH<sub>2</sub>)Cl<sub>2</sub>] display antifungal activity.

Received 2nd February 2016  
Accepted 21st May 2016

DOI: 10.1039/c6ra03068h

www.rsc.org/advances

## Introduction

In the past, transition metals and medicinal applications were thought to be mutually exclusive. Today, the therapeutic applications of transition metal complexes is an underdeveloped area of research. These complexes offer a great diversity in their application. Not only do they have anti-cancer properties but they have also been used as anti-inflammatory, anti-diabetic, anti-bacterial and anti-fungal compounds.<sup>1–3</sup> The development of transition metal complexes as drugs is not an easy task; considerable effort is required to get a compound of

interest. Besides all these limitations and side effects, coordination compounds are still the most widely used chemotherapeutics in a way that was unimaginable a few years ago.

The number of platinum complexes that show antitumor activity is still rapidly growing, because of attempts to find complexes with their greater therapeutic potency and lower toxicity than existing clinical drugs. As a consequence, the attention has turned to other platinum group metals, like ruthenium, osmium, iridium and rhodium. A special attention has been focused on ruthenium compounds because they exhibit cytotoxicity against cancer cells and no cross-resistance with cis-platin.<sup>4</sup> Ruthenium complexes demonstrate similar ligand exchange kinetics to those of platinum(II) antitumor drugs already used in clinical treatment, while displaying only low toxicity.<sup>5</sup> This is partially due to the ability of ruthenium complexes to mimic the binding of iron to molecules of biological significance, exploiting mechanisms the organism has evolved for iron transport.<sup>6–8</sup> The most promising metal-based anticancer drug candidates in clinical trials are the Ru(III) containing imidazolium *trans*-[tetrachlorido(1*H*-imidazole)(dimethylsulfoxide)ruthenate(III)] (NAMI-A) and *trans*-[tetrachloridobis(1*H*-indazole)ruthenate(III)] complexes (KP1019).<sup>9,10</sup> KP1019 is efficient in colorectal carcinoma models, while NAMI-A is an antimetastatic agent which can affect the motility of cancer cells.<sup>11,12</sup> The mode of action and the intracellular targets of Ru(III) complexes are not exactly known. There are many

<sup>a</sup>Laboratory of Intermolecular Interactions, Faculty of Chemistry, University of Gdansk, W. Stwosza 63, 80-308 Gdansk, Poland. E-mail: agnieszka.chylewska@ug.edu.pl; mariusz.makowski@ug.edu.pl; Fax: +48 523 50 12; Tel: +48 58 523 50 55

<sup>b</sup>Laboratory of Biologically Active Compounds, Intercollegiate Faculty of Biotechnology, University of Gdansk and Medical University of Gdansk, Abrahama 58, 80-307 Gdansk, Poland

<sup>c</sup>Faculty of Pharmacy with Subfaculty of Laboratory Medicine, Al. Hallera 107, 80-416 Gdansk, Poland

<sup>d</sup>Laboratory of Molecular Virology, Intercollegiate Faculty of Biotechnology, University of Gdansk and Medical University of Gdansk, Kladki 24, 80-822 Gdansk, Poland

<sup>e</sup>Institute of Biotechnology and Molecular Medicine, Trzy Lipy 3 St., 80-172 Gdańsk, Poland

† Electronic supplementary information (ESI) available: Supplementary data containing infrared spectra of Ru(III) complexes, spectrophotometric titration curves and Hyperchem data associated with this article can be found. See DOI: 10.1039/c6ra03068h



investigations suggesting that the intravenously injected drugs can be transported mainly by the serum albumin and/or transferrin in the blood plasma.<sup>13–16</sup> The reduction of Ru(III) compounds in cytosol leads to the kinetically more labile and more reactive Ru(II) compounds. This is a result of the reductive atmosphere in tumor cells due to fast anabolic processes.<sup>9,17</sup> DNA and cellular proteins like kinases or other enzymes were suggested as intracellular targets.<sup>18,19</sup>

Our careful literature search indicated that ruthenium(III) complexes with pyrazinamide (*PZA*) analogue in which the amide moiety in a second position of the pyrazine ring has been replaced by thiocarboxamide group (*PTCA*), amidoxime moiety (*PAOX*), 2-pyridyl ring (*DPP*) and amine group (*ABMAP*), respectively, (Fig. 1) have not been very well recognized and their physicochemical and biological properties have been insufficiently studied.

Due to the low number of scientific publications and information on analogues of *PZA*, it is believed that the results of our research shown in this paper will be an original and significant contribution to the development of the field.

It is known that pyrazine ring is a part of polycyclic derivative and plays important biological and industrial roles.<sup>20</sup> The pharmacological activities of the pyrazine derivatives vary and include substances with multidirectional actions. A low toxicity of these groups of compounds allows us to use them as a pharmacophore in designing new compounds to be used as drugs. The discovery of natural pyrazine derivatives, that

showed the pharmacological effect, initiated the search for novel and more effective synthetic compounds exhibiting biological activities. There is a number of substances having anti-tuberculous<sup>21,22</sup> and antibacterial activities,<sup>23,24</sup> antifungal and cytotoxic effects,<sup>25,26</sup> respectively, in the group of synthetic pyrazine derivatives. In addition, the compounds belonging to this group display antioxidant,<sup>27</sup> antiproliferative,<sup>28</sup> and antitumor activities.<sup>29</sup>

The compounds containing S, N and N, O donor atoms are important owing to their significant antifungal, antibacterial and anticancer activities.<sup>30,31</sup> Cytotoxicity can be further improved by using ligands with O, N or N, N donor systems. A type of chelating ligands does not only have an influence on the biological properties but also bears impact on the stability of the formed complex.<sup>32–34</sup> Furthermore, the ligand can modify the interaction with different biomolecules such as albumin, transferrin or various cellular proteins. It is well known that some drugs have increased their activities when administered as metal complexes rather than administered as free organic compounds.<sup>35–38</sup> A large number of reports are available on the chemistry and biological activity of transition metal complexes containing O, N and S, N donor atoms, but reports on Ru(III) coordination compounds are limited.<sup>39,40</sup>

As a part of our studies about simple inorganic models of interest for the development of the bioinorganic chemistry of ruthenium, we have started the investigations on Ru(III) complexes with *PAOX*, *PTCA*, *DPP* and *ABMAP*. The selected

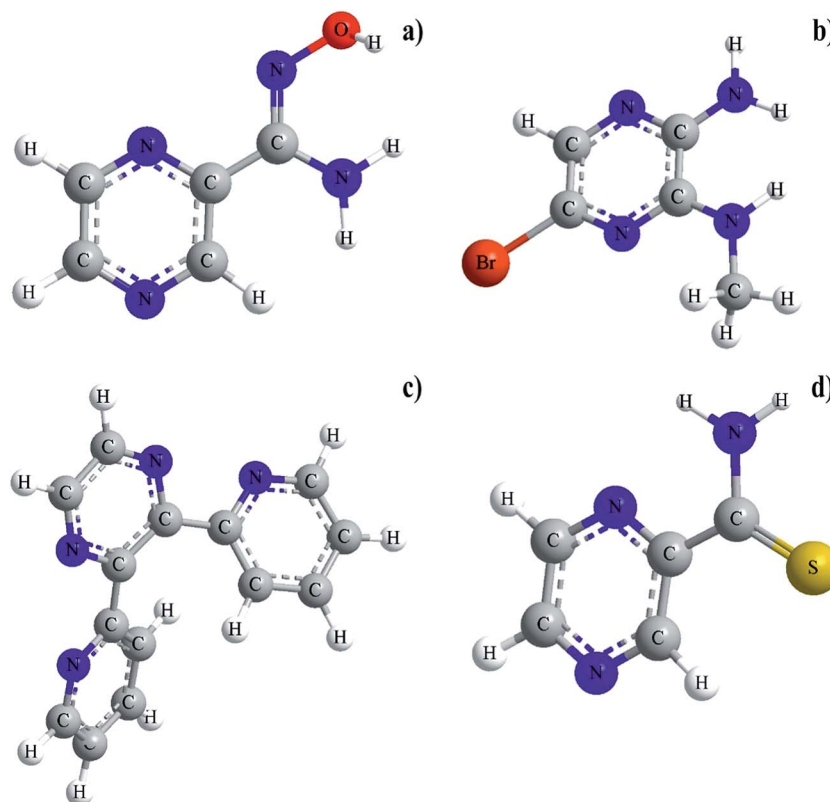


Fig. 1 Structures of selected pyrazine derivatives: (a) pyrazine-2-amidoxime (*PAOX*), (b) 2-amino-5-bromo(3-methylamino)pyrazine (*ABMAP*), (c) 2,3-bis(2-pyridyl)pyrazine (*DPP*), (d) pyrazine-2-thiocarboxamide (*PTCA*).



analogues of *PZA* appear to be suitable models due to the preference of ruthenium for oxygen and nitrogen donor atoms in biological systems.

Recently, our research group have initiated a series of studies on the effect of different substituents at the second position of the pyrazine ring on the stereochemistry of the complexes formed. We observed the direct relation between the structure of a selected organic derivative as ligand and biological activity of the obtained coordination compounds. In this work, the chelation mechanism of selected pyrazine derivatives with Ru(III) was studied in order to show and understand the biosynthetic role of ruthenium(III) ion *in vivo* as well as to develop its bioactive compounds. The stabilities of Ru(III) complexes in aqueous solution have never been investigated using the spectroscopic method. Herein, the results of the first spectrophotometric determination of the gradual equilibrium constants of *PAOX*, *PTCA*, *DPP* and *ABMAP* with Ru(III) in acetonitrile (MeCN) are presented. The obtained data clearly demonstrated the formation of 1 : 1 and 1 : 2 metal to ligand complexes for all investigated compounds. Additionally, to the best of our knowledge, pyrazine-2-amidoxime, pyrazine-2-thiocarboxamide, and 2-amino-5-bromo-3-(methylamino) pyrazine have never been employed as ligands in transition metal complexes. Here, new ruthenium(III) chloride coordination compounds with pyrazine derivatives, together with the preliminary studies of their biological properties, are shown and described. It was shown in our previous studies that structures of the ligands had an important impact on the stability and the ability to inhibit microbial proliferation of compounds used.<sup>41–44</sup> We believe the results of our studies will be helpful to further understand the binding mechanisms and can provide very important information for designing a new type of highly effective antifungal drugs. The obtained Ru(III) complexes are considered to be potential prodrugs; the knowledge of their speciation and the most plausible chemical forms in aqueous solution in the biologically relevant pH range is a mandatory prerequisite for understanding the alternations in their biological activity.

The stability of Ru(III) complexes with selected pyrazine derivatives has never been investigated in aqueous solution with the use of spectroscopic method. Herein, the results of the first spectrophotometric determination of the gradual equilibrium constants of *PAOX*, *PTCA*, *DPP* and *ABMAP* with Ru(III) in acetonitrile (MeCN) and in aqueous solution are presented. A several researchers investigated stability of similar Ru(III) complexes, but they used solvolysis or hydrolysis of synthesized coordination compounds and they measured kinetic parameters of reactions.<sup>45–49</sup> The main goal of our present studies is to find and explain the influence of metal ion on spectral properties of selected pyrazine derivatives. We observed the complex formation of defined stoichiometry (1 : 1 and 1 : 2) during addition small amount of metal ion to ligand solution and recorded spectral changes. This spectral changes, *i.e.* increase/decrease of intensity, appearance of isosbestic points, and batho- or hypsochromic effects are the results of interactions between the hard acid Ru(III) ion and donor atoms of ligand. Based on the results from spectrophotometric measurements

the values of gradual and cumulative formation constants for Ru(III) complexes were determined. To our knowledge, the stability of Ru(III) complexes in both aqueous and MeCN solutions has never been investigated by using spectrophotometric procedure presented in this paper. Consequently, here we report the results of the first spectrophotometric determination of the gradual equilibrium constants of the ruthenium(III) complexes with analogues of *PZA*.

The main purpose of the present work is fully characterization of Ru(III) complexes with selected analogues of pyrazinamide in the solid state and in solution and the preliminary studies of their biological properties. Moreover, we focused also on the determination of the influence of the structure ligand on the stability and the ability to inhibit microbial proliferation of compounds used. We believe the results of our studies will be helpful to further understand the binding mechanisms and can provide very important information for designing a new type of highly effective antifungal drugs. The obtained Ru(III) complexes are considered to be potential prodrugs; the knowledge of their speciation and the most plausible chemical forms in aqueous solution in the biologically relevant pH range is a mandatory prerequisite for understanding the alternations in their biological activity.

## Results and discussion

The synthesized Ru(III) complexes are non-hygroscopic (stable at room temperature) and in the form of amorphous solids but, unfortunately, crystals suitable for X-ray measurements were not available. Melting points of the newly synthesized ruthenium(III) coordination compounds were in the range of 256–280 °C. The complexes were soluble in water and in common organic solvents like acetonitrile and dimethyl sulfoxide. The results of elemental analysis and analytical data of the examined coordination compounds suggest that the metal to ligand ratio of the complexes is 1 : 2 stoichiometry of the type  $[\text{RuCl}(\text{py})_2(\text{OH}_2)]\text{Cl}$  for *PTCA* and *PAOX* and  $[\text{RuCl}_2(\text{py})_2]\text{Cl}$  for *ABMAP*, 1 : 1 stoichiometry of the type  $[\text{RuCl}(\text{py})(\text{OH}_2)_3]\text{Cl}$  for *DPP*, respectively, where *py* stands for bidentate pyrazine derivatives. Selected physicochemical data are given in Table 1.

The presence of water molecules in the compounds is deduced from elemental analysis, IR spectra and thermal analysis (TG). The presence of chloride counter ion in the Ru(III) complexes was detected with a few drops of the concentrated silver nitrate reagent and the appearance of the white precipitate.

### Infrared spectra studies

The infrared absorption bands are one of the most important tools of analysis used to determine the mode of coordination. The IR spectra of free ligands were compared with the spectra of their Ru(III) complexes. Strong bands in the range of 3403–3437  $\text{cm}^{-1}$  region in the spectra of coordination compounds studied with *PTCA*, *PAOX* and *DPP* were assigned to a  $\nu(\text{O-H})$  stretching and suggested the presence of water molecules in the coordination sphere of these compounds. New bands (Table 2) were



Table 1 Analytical data and physical properties of Ru(III) complexes

Complex	Colour	M. wt. (g mol <sup>-1</sup> )	Melting point (°C)	Yield (%)	% Found (calcd.)			
					C	H	N	S
[RuCl( <i>PTCA</i> ) <sub>2</sub> (OH <sub>2</sub> )Cl <sub>2</sub> ] (C <sub>10</sub> H <sub>12</sub> Cl <sub>3</sub> N <sub>6</sub> O <sub>2</sub> Ru)	Dark brown	503.80	275	96	23.84 (23.80)	2.40 (2.45)	16.68 (16.65)	12.73 (12.70)
[RuCl( <i>DPP</i> )(OH <sub>2</sub> ) <sub>3</sub> ]Cl <sub>2</sub> (C <sub>14</sub> H <sub>16</sub> Cl <sub>3</sub> N <sub>4</sub> O <sub>3</sub> Ru)	Black	495.70	280	88	33.90 (33.92)	3.23 (3.23)	11.28 (11.28)	—
[RuCl <sub>2</sub> ( <i>ABMAP</i> ) <sub>2</sub> ]Cl (C <sub>10</sub> H <sub>14</sub> Br <sub>2</sub> Cl <sub>3</sub> N <sub>8</sub> Ru)	Black green	613.50	262	83	19.55 (19.58)	2.26 (2.30)	18.23 (18.26)	—
[RuCl( <i>PAOX</i> ) <sub>2</sub> (OH <sub>2</sub> )Cl <sub>2</sub> ] (C <sub>10</sub> H <sub>14</sub> Cl <sub>3</sub> N <sub>8</sub> O <sub>3</sub> Ru)	Navy blue	501.70	256	79	23.94 (23.90)	2.81 (2.79)	22.33 (22.31)	—

Table 2 Prominent IR absorption peaks of ruthenium(III) complexes in the region 4000–400 cm<sup>-1</sup>

Complex	$\nu(\text{OH})$	$\nu(\text{N-H})$	$\nu(\text{C=N})$	$\nu(\text{C-N})$	$\nu(\text{Ru-N})$	$\nu(\text{Ru-Cl})$
[RuCl( <i>PAOX</i> ) <sub>2</sub> (OH <sub>2</sub> )Cl <sub>2</sub> ]	3403	3160	1642	1036	646	524
[Ru( <i>PTCA</i> ) <sub>2</sub> (OH <sub>2</sub> ) <sub>2</sub> ]Cl <sub>3</sub> ·3H <sub>2</sub> O	3419	3065	1579	1039	580	471
[Ru( <i>ABMAP</i> ) <sub>3</sub> ]Cl <sub>3</sub>	—	3403	1550	1347	589	479
[RuCl( <i>DPP</i> )(OH <sub>2</sub> ) <sub>4</sub> ]Cl <sub>2</sub> ·7H <sub>2</sub> O	3437	—	1634	1391	586	494

observed at the far IR region between 646 and 471 cm<sup>-1</sup> for all chloride Ru(III) complexes with pyrazine derivatives, which were absent in the spectrum of free ligands. These bands have been ascribed to prominent peak of stretching frequencies of  $\nu(\text{Ru-N})$  and  $\nu(\text{Ru-Cl})$  vibrations, respectively.

In the case of [RuCl(*PAOX*)<sub>2</sub>(OH<sub>2</sub>)Cl<sub>2</sub>], a band at 3160 cm<sup>-1</sup> in the spectrum of the complex can be attributed to the stretching vibration of NH<sub>2</sub> moiety (see Fig. S1 of the ESI<sup>†</sup>). Moreover, the characteristic absorption at 1659 cm<sup>-1</sup> in the free pyrazine-2-amidoxime can be assigned to  $\nu(\text{C=N})$  stretching vibrations of azomethine nitrogen.<sup>50,51</sup> After complexation, this frequency was observed to be shifted to lower wave numbers (1642 cm<sup>-1</sup>), which confirmed the involvement of a nitrogen atom in bonding with ruthenium(III) ion. The infrared spectrum of free *PAOX* showed a sharp band at 953 cm<sup>-1</sup> due to  $\nu(\text{N-O})$  stretching vibrations of oxime group. The bathochromic effect of frequency (844 cm<sup>-1</sup>) was observed after synthesis, implying the possibility of coordination by a nitrogen atom of this moiety.

In the spectrum of pyrazine-2-thiocarboxamide (see Fig. S2 of the ESI<sup>†</sup>) the bands at 3341 cm<sup>-1</sup>, and 3239 cm<sup>-1</sup> are ascribed to symmetric and antisymmetric stretching vibrations of NH<sub>2</sub> group, respectively. In comparison with the spectrum of the Ru(III) complex, these bands disappeared, which confirmed the participation of a nitrogen atom in the complexation of metal ion. The strong and sharp band at 1607 cm<sup>-1</sup> in the case of pyrazine-2-thiocarboxamide can be attributed to  $\nu(\text{C=N})$  stretching vibrations. The significant bathochromic effect of this frequency after synthesis implied a possibility of complexation by the nitrogen of the azomethine group.

The characteristic absorption of the azomethine group appeared at 1653 cm<sup>-1</sup> in the spectrum of 2,3-bis(2-pyridyl)pyrazine (Fig. S3 of the ESI<sup>†</sup>). This frequency was observed to be shifted to lower wave numbers (1634 cm<sup>-1</sup>) after complexation, which confirmed the involvement of a nitrogen atom in bonding with metal ion. The strong band at 1391 cm<sup>-1</sup> is

designated to  $\nu(\text{C-N})$  stretching modes of vibrations, which is consistent with the assignment for aromatic compounds.<sup>52</sup> In the spectrum of [RuCl(*DPP*)(OH<sub>2</sub>)<sub>3</sub>]Cl<sub>2</sub> all characteristic bands, which can be attributed to aromatic stretching vibrations in the region between 1500–1000 cm<sup>-1</sup>, were absent in our measurements, indicating that a nitrogen atom of pyridyl ring was involved in complexation of ruthenium(III) ion.

The strong, sharp band at 3438 cm<sup>-1</sup> in the spectrum of 2-amino-5-bromo-3-(methylamino)pyrazine can be attributed to  $\nu(\text{NH}_2)$  stretching vibrations (Fig. S4 of the ESI<sup>†</sup>). The bathochromic shift of this frequency to 3403 cm<sup>-1</sup> after synthesis implied the possibility of complexation by the nitrogen atom of the amine group. Two bands at 1586 cm<sup>-1</sup> and 1383 cm<sup>-1</sup> occurred in the spectrum of *ABMAP*, which can be ascribed to  $\nu(\text{N-H})$  and  $\nu(\text{C-N})$  stretching vibrations, respectively. In comparison with its Ru(III) complex, these bands were shifted to 1550 cm<sup>-1</sup> and 1347 cm<sup>-1</sup>, respectively. This observation suggested that *ABMAP* coordinated Ru(III) ion by two nitrogen atoms of amine and methylamine groups, respectively.

The analysis of presented IR spectra of studied complexes in this work leads to a conclusion that selected pyrazine derivatives behave as bidentate ligands. In case of pyrazine-2-amidoxime complex, a ligand is coordinated to the metal ion by azomethine nitrogen and nitrogen of oxime groups. In the [RuCl(*PTCA*)<sub>2</sub>(OH<sub>2</sub>)Cl<sub>2</sub>] the pyrazine-2-thiocarboxamide is bonded to the Ru(III) ion through the amine and azomethine nitrogen atoms, respectively. And the binding set of Ru(III) complex with 2,3-bis(2-pyridyl)pyrazine includes nitrogen of the azomethine group and pyridyl ring. In the [RuCl<sub>2</sub>(*ABMAP*)<sub>2</sub>]Cl, the ruthenium(III) ion is coordinated by two nitrogen atoms of amine and methylamine groups, respectively. This means that there were more energetically favorable five-membered rings formed during the complexation process, which was consistent with indicated coordination sites.



### Proton nuclear magnetic resonance spectra studies

Although Ru(III) complexes are paramagnetic, proton nuclear magnetic resonance spectroscopy can provide important structural information for such compounds.<sup>53,54</sup> The <sup>1</sup>H NMR spectral data of ruthenium(III) complexes with selected pyrazine derivatives were recorded in DMSO-d<sub>6</sub> (Fig. S5–S8 of ESI†). The intensities of all resonance lines were determined. The assignment of the characteristic signals was performed by comparison with spectra of similar Ru(III) complexes.<sup>55</sup> The presented <sup>1</sup>H NMR spectra have several broad peaks, in accordance with the presence of paramagnetic Ru(III) metal ions.

The following conclusions can be derived by comparing the spectra of ligands and their coordination compounds. The signal due to N–H protons appeared at 7.61 ppm in the case of [RuCl<sub>2</sub>(ABMAP)<sub>2</sub>]Cl and 8.14 ppm for [RuCl(PTCA)<sub>2</sub>(OH<sub>2</sub>)<sub>2</sub>]Cl<sub>2</sub>. The downfield shifts of this signal in Ru(III) complexes occurred. This is correlated to the decrease of electron density and the deshielding of proton because of participation of amine and azomethine groups upon coordination which was observed in earlier report for Ru(III) complexes.<sup>56</sup> Furthermore, in the [RuCl<sub>2</sub>(ABMAP)<sub>2</sub>]Cl, the disappearance of signal due to N–H proton in the third position of pyrazine ring indicated participation of this group in chelation process. In the case of PAOX signal correspond to N–H proton occurred at 5.25 ppm, which remains unchanged in their ruthenium(III) complex. This observation confirmed that amine group is not involved in complexation process of metal ion. The peaks observed and in the range 8.93–8.74 ppm and 7.30–7.03 ppm in the spectra of Ru(III) complexes are assigned to the presence of aromatic proton of pyrazine ring. The downfield shifts of peaks correspond to H6 proton of pyrazine ring and H2 proton of pyridyl ring is correlated to the decrease electron density caused by participation of nitrogen atoms of azomethine group and pyridyl ring. The position of protons correspond well with the proposed structure of Ru(III) complexes and were assigned in view of earlier reports.<sup>57,58</sup>

### Electrospray ionization mass spectrometry analysis (ESI-MS)

Mass spectroscopy, which is mainly used in the analysis of biomolecules, has been increasingly applied as a powerful tool of structural characterization in coordination chemistry.<sup>59–61</sup> The ESI-MS spectra of Ru(III) complexes dissolved in acetonitrile are comparison with simulated data and the obtained results are presented in Fig. S9–S12 of ESI.† The mass spectra of compounds studies were recorded in the positive mode and in the range of  $m/z = 50–800$ . The molecular peaks for the complexes of Ru(III) were observed at  $m/z = 501.9, 503.8, 495.9$  and  $612.8$  for PAOX, PTCA, DPP and ABMAP, respectively which corresponding to the actual molecular weights of these complexes. For all Ru(III) compounds studies, experimental and simulated data are in good agreement, which well correspond with previous report for similar type of complexes.<sup>62</sup> The presented results of ESI-MS studies of each Ru(III) complexes with pyrazine derivatives support the proposed structure of the coordination compounds.

### Electronic spectra of complexes synthesized

The electronic absorption spectra of Ru(III) complexes with selected pyrazine derivatives were recorded in acetonitrile in the range 250–700 nm (Fig. 2). UV-Vis spectral data for synthesized Ru(III) complexes were given in Table 3.

The ground state of ruthenium(III) ion ( $t_{2g}^5$  configuration) is  $^2T_{2g}$ . The first excited doublet levels in order of increasing energy are  $^2A_{2g}$  and  $^2T_{1g}$  which arise from  $t_{2g}^4 e_g^1$  configuration.<sup>63,64</sup> These Ru(III) complexes are low spin ( $t_{2g}^5$ ) with one unpaired electron; hence the bands observed can attributed to ligand field transitions for ruthenium(III) with  $t_{2g}^5$  configuration. In the octahedral ligand field symmetry the spectrum of ruthenium(III) should show the spin-allowed d–d bands in the visible region.<sup>65</sup> According to Tanabe–Sugano energy matrices<sup>66,67</sup> for d<sup>5</sup>-octahedral geometry, the bands appearing in the range of 18 657–20 202 and 21 276–26 178 cm<sup>-1</sup> were assigned to  $^2T_{2g} \rightarrow ^2A_{1g}$  or  $^2T_{1g}$  and  $^2T_{2g} \rightarrow ^2E_g$ , respectively. The bands of high intensity in the range 31 746–37 174 cm<sup>-1</sup> were also observed. These bands were assigned to  $\pi \rightarrow \pi^*$  and  $n \rightarrow \pi^*$  intra-ligand charge transfer. The ligand field parameters could be estimated by using the energies  $^2T_{2g} \rightarrow ^2A_{1g}$  and/or  $^2T_{1g}$ , and  $^2T_{2g} \rightarrow ^2E_g$  transitions, and the Tanabe–Sugano energy matrices for d<sup>5</sup>-octahedral geometry.

The values of splitting parameter ( $\Delta_0$ ) in the range 21 560–31 631 cm<sup>-1</sup> were obtained. The values of Racah parameter of interelectronic repulsion ( $B$ ) in the range 616–691 cm<sup>-1</sup> and nephelauxetic parameter ( $\beta$ ) in the range 0.64–0.72 were found (see Table 3). The ligand field parameters ( $\Delta_0, B, \beta$ ) are close to those reported for similar octahedral ruthenium(III) complexes.<sup>68,69</sup> The values of the splitting parameters placed the pyrazine derivatives in the middle range of spectrochemical series and provide reassurance that these ligands were coordinated to the Ru(III) ion through the nitrogen donor atoms. The  $B$  values for ruthenium(III) complexes (lower than that of free ion) indicate a considerable orbital overlap with a strong covalent metal–ligand bond.<sup>70</sup> According to Jorgensen,<sup>65</sup> a decrease in  $B$ -value is associated with the reduction in the nuclear charge on

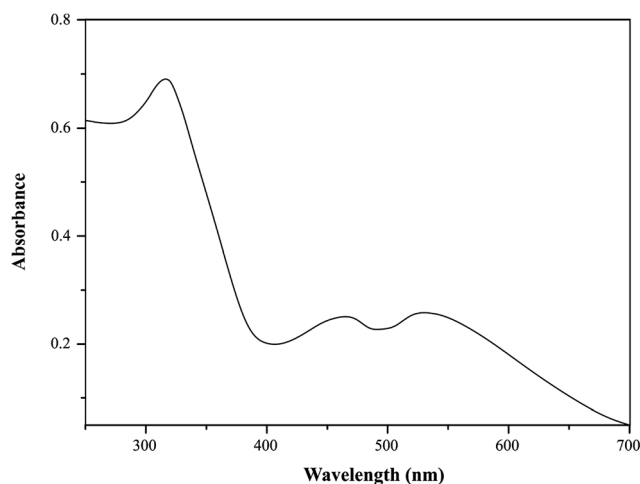


Fig. 2 The representative electronic spectrum of [RuCl(DPP)(OH<sub>2</sub>)<sub>3</sub>]Cl<sub>2</sub> recorded in acetonitrile.



Table 3 Electronic spectral data and ligand fields parameters (cm<sup>-1</sup>) for the prepared Ru(III)–pyrazine derivatives complexes in MeCN<sup>a</sup>

Complex	$\nu_1$ ( ${}^2T_{2g} \rightarrow {}^2A_{1g}, {}^2T_{1g}$ )	$\nu_2$ ( ${}^2T_{2g} \rightarrow {}^2E_g$ )	$\nu_3$ ( $\pi-\pi^*, n-\pi^*$ )	$\nu_2/\nu_1$	$\Delta_0$	$B$	$\beta$	$C$
[RuCl( <i>PTCA</i> ) <sub>2</sub> (OH <sub>2</sub> )Cl] <sub>2</sub>	19 194	24 038	31 746	1.25	23 261	638	0.66	2552
[RuCl( <i>DPP</i> )(OH <sub>2</sub> ) <sub>3</sub> ]Cl <sub>2</sub>	18 657	21 276	32 258	1.14	21 560	616	0.64	2464
[RuCl <sub>2</sub> ( <i>ABMAP</i> ) <sub>2</sub> ]Cl	19 048	24 509	32 787	1.29	29 450	691	0.72	2764
[RuCl( <i>PAOX</i> ) <sub>2</sub> (OH <sub>2</sub> )Cl] <sub>2</sub>	20 202	26 178	37 174	1.31	31 631	639	0.66	2556

<sup>a</sup> The ligand field parameters ( $\Delta_0$ ,  $B$ ,  $C$  and  $\beta$ ) were calculated by data obtained from the experimental UV-Vis spectra of ruthenium(III) complexes and Tanabe–Sugano diagram for d<sup>5</sup> octahedral geometry.<sup>54</sup>

the cation and an increasing tendency to be reduced. It is apparent that the  $\beta$  parameter depends greatly on the electro-negativity of the donor atoms and the ligand structure. The values of nephelauxetic parameter ( $\beta$ ) are also less than one and show that selected ligands are middle nitrogen donor series.

### Conductance

The conductivity values of 10<sup>-3</sup> M solutions of the synthesized complexes were carried out in water at 25 °C and presented in Table 4. All systems studied have the conductivity in the range 686.50–127.5  $\mu\text{S cm}^{-1}$ . These values indicate that Ru(III) complexes are electrolytes. The conductivities of 10<sup>-3</sup> M solutions of NiCl<sub>2</sub> and NaCl in water were also measured as 713.00 and 133.70  $\mu\text{S cm}^{-1}$ , respectively. These values are approximate to the conductivity values of synthesized complexes. It means that the examined coordination compounds are of 1 : 1 and 1 : 2 electrolyte types as compared to NaCl and NiCl<sub>2</sub> solutions, respectively. These results confirmed that one or two chloride anions were counter ions in the coordination spheres of the ion complexes studied in this work.<sup>71</sup>

### Thermal analysis

Thermal analysis provides significant information about the stability and distribution of water molecules in the coordination sphere of metal complexes. In case of *PTCA* and *PAOX* complexes of the type [RuCl(*py*)<sub>2</sub>(OH<sub>2</sub>)]Cl and *DPP* of type [RuCl(*py*)(OH<sub>2</sub>)<sub>3</sub>]Cl, respectively, decomposition involved three steps. The TG curve of [RuCl<sub>2</sub>(*ABMAP*)<sub>2</sub>]Cl showed two main consecutive steps of mass loss. In the argon atmosphere the mass loss in the temperature range 125–180 °C corresponds to the loss of coordinated water molecule. The second step was

Table 4 Conductance values of Ru(III) complexes with pyrazine derivatives were obtained in water at concentration of 1.00 × 10<sup>-3</sup> mol L<sup>-1</sup>. All results were determined at 25 °C

Compound	Conductance ( $\mu\text{S} \cdot \text{cm}^{-1}$ )
[RuCl( <i>PAOX</i> ) <sub>2</sub> (OH <sub>2</sub> )Cl] <sub>2</sub>	686.5
[RuCl( <i>PTCA</i> ) <sub>2</sub> (OH <sub>2</sub> )Cl] <sub>2</sub>	611.10
[RuCl( <i>DPP</i> )(OH <sub>2</sub> ) <sub>3</sub> ]Cl <sub>2</sub>	580.60
[RuCl <sub>2</sub> ( <i>ABMAP</i> ) <sub>2</sub> ]Cl	127.50
NaCl	133.70
NiCl <sub>2</sub>	713.00

due to the removal of volatilization of appropriate pyrazine derivative and hydrochloride molecules together with chlorine (Cl<sub>2</sub>) gas moiety fragment and it occurred in the temperature range 180–460 °C. At the last step, as the final product, stable metal oxides such as Ru<sub>2</sub>O<sub>3</sub> (sometimes even RuO) were found above 750 °C as carbonaceous matter (Table 5). In all cases, the DTG study reveals that all the decomposition stages were exothermic in nature.

### Electrochemical results

Ru(III)/Ru(II) reduction potentials change with ligand environment and is thought to be very important for possible antitumor properties of a compound. The redox behavior of the ruthenium(III)–pyrazine derivative complexes was studied in acetonitrile solution at a platinum working electrode. Acetonitrile was selected as a solvent because of its well-known<sup>72,73</sup> coordination ability with Ru(II) or Ru(III) centers. The relevant electrochemical data were summarized in Table 6 and voltammograms were shown in Fig. 3.

[RuCl(*PAOX*)<sub>2</sub>(OH<sub>2</sub>)Cl]<sub>2</sub> and [RuCl(*DPP*)(OH<sub>2</sub>)<sub>3</sub>]Cl<sub>2</sub> complexes exhibit two clear redox systems. On the anodic side reversible oxidations are observed and on the cathodic side, reversible redox couples. These redox systems can be assigned to the ruthenium(III)–ruthenium(IV) (positive potentials) and ruthenium(III)–ruthenium(II) (negative potentials) couples, respectively. Both the redox responses are reversible, as reflected in the equality of the anodic peak current ( $I_{pa}$ ) with the cathodic peak current ( $I_{pc}$ ). Though the peak-to-peak separation ( $\Delta E_p$ ) is slightly larger (0.08 V) than ideally expected for a reversible electron transfer process.<sup>74</sup> No changes in the  $\Delta E_p$  values were observed in relations to changes in the scan rate.

On the basis of the above-mentioned results, [RuCl(*PTCA*)<sub>2</sub>(OH<sub>2</sub>)Cl]<sub>2</sub> and [RuCl<sub>2</sub>(*ABMAP*)<sub>2</sub>]Cl exhibit different behaviors. The reversible reduction process (Ru<sup>III</sup> → Ru<sup>II</sup>,  $\Delta E_p = 0.429$  V for complex with *PTCA* as ligand, and 0.292 V for complex with *DPP*) on cyclic voltammograms for these both complexes was observed. However, the nature of [RuCl(*PTCA*)<sub>2</sub>(OH<sub>2</sub>)Cl]<sub>2</sub> voltammogram showed the irreversible process of oxidation in high, positive potentials. In the second case, for [RuCl<sub>2</sub>(*ABMAP*)<sub>2</sub>]Cl complex, cyclic voltammetry (CV) indicated additional reduction process in negative potentials, which could be ascribed to the reversible ligand reduction ( $\Delta E_p = 0.436$  V).



Table 5 Data and thermal decomposition of Ru(III) complexes with selected pyrazine derivatives

Complex	Temp. range	% mass loss observed (calc.)	Probable composition of expelled group/residue
[RuCl( <i>PTCA</i> ) <sub>2</sub> (OH <sub>2</sub> )Cl] <sub>2</sub>	125–140	3.50 (3.57)	Loss of lattice water
	180–400	76.55 (76.62)	Loss of volatilization of two <i>PTCA</i> and HCl molecules together with chlorine (Cl <sub>2</sub> ) gas moiety fragment
[RuCl( <i>DPP</i> )(OH <sub>2</sub> ) <sub>3</sub> Cl] <sub>2</sub>	>750	19.95 (19.81)	Residue mass as ruthenium oxides
	140–180	10.79 (10.89)	Loss of three lattice water
[RuCl( <i>PAOX</i> ) <sub>2</sub> (OH <sub>2</sub> )Cl] <sub>2</sub>	240–440	68.28 (68.97)	Loss of volatilization of one <i>DPP</i> and HCl molecules together with chlorine (Cl <sub>2</sub> ) gas moiety fragment
	>765	20.93 (20.14)	Residue mass as ruthenium oxides
[RuCl <sub>2</sub> ( <i>ABMAP</i> ) <sub>2</sub> Cl]	125–150	3.51 (3.59)	Loss of lattice water
	190–460	76.30 (76.24)	Loss of volatilization of two <i>PAOX</i> and HCl molecules together with chlorine (Cl <sub>2</sub> ) gas moiety fragment
[RuCl <sub>2</sub> ( <i>ABMAP</i> ) <sub>2</sub> Cl]	>760	20.19 (20.17)	Residue mass as ruthenium oxides
	260–600	83.12 (83.42)	Loss of volatilization of two <i>ABMAP</i> and HCl molecules together with chlorine (Cl <sub>2</sub> ) gas moiety fragment
	>780	16.88 (16.58)	Residue mass as ruthenium oxides

Table 6 Electrochemical redox data of ruthenium(III) complexes in acetonitrile (TBAP 0.1 M, scan rate 50 mV s<sup>-1</sup>, 20 ± 0.1 °C)<sup>a</sup>

Voltammetric data					
Complex	Reduction, Ru <sup>III</sup> /Ru <sup>II</sup>				
	Potential [V]				
	<i>E</i> <sub>pa</sub>	<i>E</i> <sub>pc</sub>	Δ <i>E</i> <sub>p</sub>	<i>E</i> <sub>1/2</sub>	<i>I</i> <sub>pa</sub> / <i>I</i> <sub>pc</sub>
[RuCl( <i>PAOX</i> ) <sub>2</sub> (OH <sub>2</sub> )Cl] <sub>2</sub>	-1.003	-1.252	0.249	-1.127	0.357
[RuCl( <i>PTCA</i> ) <sub>2</sub> (OH <sub>2</sub> )Cl] <sub>2</sub>	-0.856	-1.285	0.429	-1.071	0.333
[RuCl <sub>2</sub> ( <i>ABMAP</i> ) <sub>2</sub> Cl]	-0.871	-1.163	0.292	-1.017	0.273
	-0.116**	-0.552**	0.436**	-0.334**	0.367**
[RuCl( <i>DPP</i> )(OH <sub>2</sub> ) <sub>3</sub> Cl] <sub>2</sub>	-0.953	-1.347	0.394	-1.150	0.308
Complex	Oxidation, Ru <sup>III</sup> /Ru <sup>IV</sup>				
	Potential [V]				
	<i>E</i> <sub>pa</sub>	<i>E</i> <sub>pc</sub>	Δ <i>E</i> <sub>p</sub>	<i>E</i> <sub>1/2</sub>	<i>I</i> <sub>pc</sub> / <i>I</i> <sub>pa</sub>
[RuCl( <i>PAOX</i> ) <sub>2</sub> (OH <sub>2</sub> )Cl] <sub>2</sub>	1.376	0.874	0.502	1.125	0.325
[RuCl( <i>DPP</i> )(OH <sub>2</sub> ) <sub>3</sub> Cl] <sub>2</sub>	1.312	0.906	0.406	1.109	0.788
[RuCl( <i>PTCA</i> ) <sub>2</sub> (OH <sub>2</sub> )Cl] <sub>2</sub>	1.302*	—	—	—	—

<sup>a</sup> Reference electrode – SCE;  $E_{1/2} = 0.5(E_{pa} + E_{pc})$  where  $E_{pa}$  and  $E_{pc}$  are anodic and cathodic peak potential, respectively;  $\Delta E_p = E_{pa} - E_{pc}$ ; \* $E_{pa}$  of [RuCl(*PTCA*)<sub>2</sub>(OH<sub>2</sub>)Cl]<sub>2</sub> is considered due to the irreversible nature of the voltammogram. \*\* Potentials of *ABMAP* ligand reduction.

### Molecular structure and analysis of bonding modes

Molecular mechanics modeling was carried out to estimate the optimal electron energies, selected structure parameters, and to confirm the possibility of the studied compounds formation. In order to ascertain the structural preferences and coordination behavior of pyrazine derivatives (L) to ruthenium(III) ion, molecular mechanics calculations on the [RuL<sub>*n*</sub>]<sup>3+</sup> species (1 < *n* < 3) were undertaken. Energy minimization was repeated several times to find the global minimum. The bond lengths and angles of all complexes were presented in Tables S1–S8,† respectively. The results of calculations have proven clear octahedral sphere of Ru(III) complexes and the formation of

stable coordination compounds. It is important to note that in all four complexes Ru–O and Ru–N bond lengths are almost the same (1.89 < *d* [Å] < 1.95), the only difference being in bond angles. The analysis of Ru–Cl bond lengths showed similar values of about 2.25 Å for complexes of Ru(III) ions with *ABMAP*, *PTCA* and *PAOX*; except for complex cation with 2,3-bis(2-pyridyl)pyrazine – [RuCl(*DPP*)(OH<sub>2</sub>)<sub>3</sub>]<sup>+</sup>, where Ru–Cl bond length is shorter, *i.e.* 1.93 Å. The bond angles in all complexes are quite near to an octahedral arrangement predicting sp<sup>3</sup>d<sup>2</sup> hybridization (Fig. 4 and S13†).

The final coordinates and their heat of formations found by the PM3 method were shown in Table S9 of the ESI.†



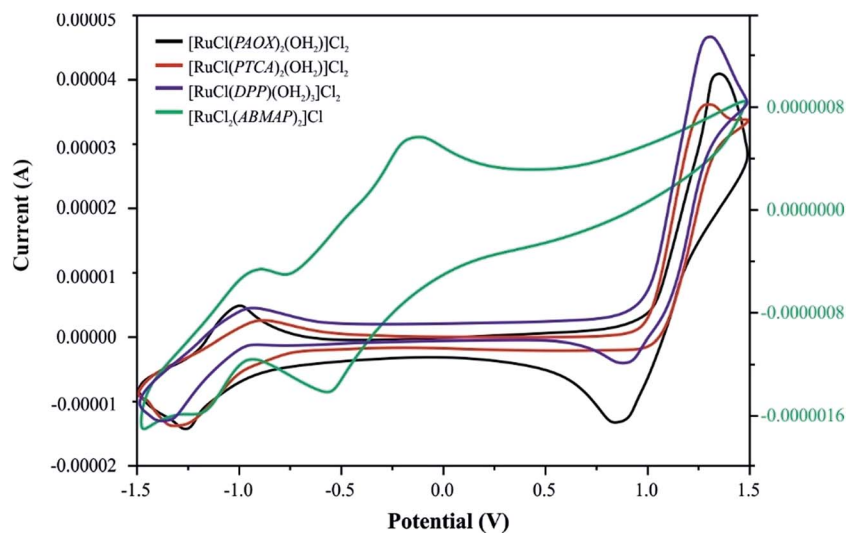


Fig. 3 Cyclic voltammograms of four Ru(III) complexes with selected pyrazine derivatives (*PAOX*, *PTCA*, *ABMAP*, *DPP*) in acetonitrile solution (0.1 M TBAP) at a scan rate of  $50 \text{ mV s}^{-1}$ .

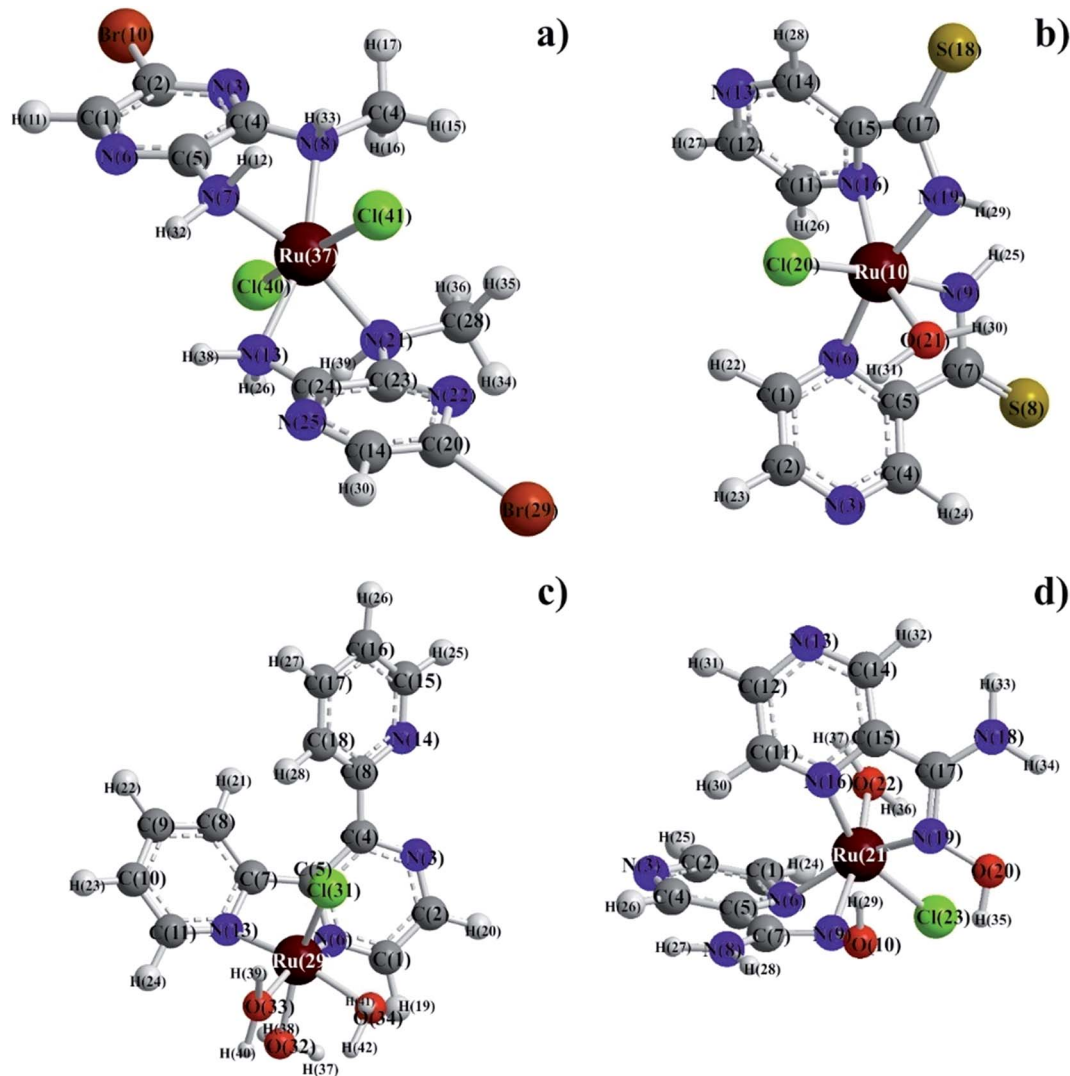


Fig. 4 Final structures of: (a)  $[\text{RuCl}_2(\text{ABMAP})_2]\text{Cl}$ , (b)  $[\text{RuCl}(\text{PTCA})_2(\text{OH}_2)]\text{Cl}_2$ , (c)  $[\text{RuCl}(\text{DPP})(\text{OH}_2)_3]\text{Cl}_2$ , (d)  $[\text{RuCl}(\text{PAOX})_2(\text{OH}_2)]\text{Cl}_2$ , respectively, found at PM3 level of semi-empirical calculations *in vacuo*.

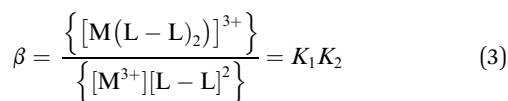
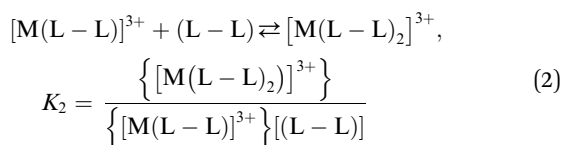
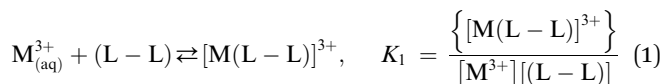


### Complexometric properties of pyrazine derivatives analogues of PZA

The presence of chromophore groups in a molecule of a ligand, whose absorption spectra change upon complexation, allows for using spectroscopy methods to study chelation process. Spectrophotometric titration is a very useful method to determine the stability constants in solution. Based on the results from spectroscopy measurements, it is possible to show a quantity of equilibria existing in a particular solution. Furthermore, this investigation can provide complete information about species formed during the titration process.

The stability constants of pyrazine derivatives complexes with ruthenium(III) ion were determined by titration of the bidentate ligand (L-L) and recorded the spectral changes in the range 200–600 nm in MeCN (Fig. 5–8) and in aqueous solution (see Fig. S14–S17 of ESI†). Water was selected as a solvent because of its crucial role in microbiological assay. The change of the solvent from water to acetonitrile was made because of its better coordination ability with ruthenium(III) ion.

The values of stability constants for investigated complexes were calculated using EQUID computer program.<sup>75</sup> This program is based on the non-linear least-square Gauss–Newton–Marquardt method for fitting procedure.<sup>75,76</sup> The gradual ( $K$ ) and cumulative ( $\beta$ ) stability constants can be described by the following eqn (1)–(3):



The presence of metal ion also influences spectral properties of the investigated ligands. The interaction of Ru(III) with

pyrazine-2-thiocarboxamide induces changes in the absorption band positions after complexation. To determine the stability constants of *PTCA* with ruthenium(III), the ligand studied was titrated by acetonitrile solution of metal chloride salt and *PTCA*. Based on the analysis of the spectrophotometric titration curves, the number of equilibria and stoichiometry of formed complex were determined (Fig. 5a). The intensities of absorption bands increase and hyperchromic effect can be also observed. At the same time a new peak appeared at 412 nm. This observation suggests the existence of metal ion interactions with hard donor atom of *PTCA* in the system studied.

Dependence of the absorbance at 251 nm to the absorbance at 239 nm Ru(III)–*PTCA* system was obtained (see Fig. 5b). Two straight sections presented on the plot confirmed two equilibria during chelation process. The dependence of absorbance at 262 nm for 2-thiocarboxamide as a function of molar ratio  $n_{Ru(III)}/n_{PTCA}$  is presented in Fig. 5c. The fitted data confirmed metal : ligand stoichiometry 1 : 2 of the complex formation process.

The results of spectrophotometric titration for Ru(III) ion with 2,3-bis(2-pyridyl)pyrazine system studied in MeCN solution have been shown in Fig. 6a. The intensities of absorption bands gradually increase and a slight hypsochromic shift can be observed. The changes in absorbance values are associated with chelation of nitrogen donor atom to ruthenium(III) cation. The *A*-diagrams (the dependence of absorbance at 233 nm as a function of absorbance at 279 nm) were plotted to illustrate specific quantity equilibria constants in arrangement studied (see Fig. 6b). The presence of two straight sections in these diagrams indicate two equilibria in the system studied. These observations are confirmed by the dependence of absorbance at 354 nm for 2,3-bis(2-pyridyl)pyrazine as a function of molar ratio  $n_{Ru(III)}/n_{DPP}$  (see Fig. 6c). The metal : ligand stoichiometry 1 : 2 in arrangement of the studied complex is formed, which is consistent with values of molar ratio equal 0.5.

During the titration process of pyrazine-2-amidoxime by the ruthenium(III) chloride in acetonitrile solution with *PAOX* a slight shift to longer wavelengths (bathochromic effect) occurred. At the same time the maximum of band at 410 nm can be observed (Fig. 7a). These effects suggest the existence of metal ion interactions with donor atom of ligand in the system studied. The *A*-diagrams were analyzed to determine the

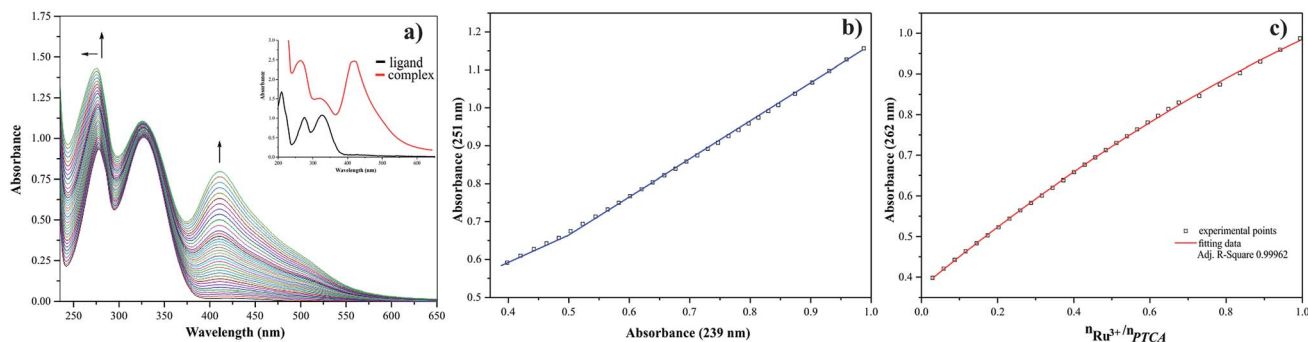


Fig. 5 (a) Spectrophotometric titration curves of pyrazine-2-thiocarboxamide ( $1.00 \times 10^{-4} \text{ mol L}^{-1}$ ) using a mixture of *PTCA* at the same concentration and  $\text{RuCl}_3$  ( $1.81 \times 10^{-3} \text{ mol L}^{-1}$ ). (b) The *A*-diagram plot for Ru(III) ion with pyrazine-2-thiocarboxamide complexation process, major stoichiometry 1 : 2. (c) Dependence of absorbance at 262 nm for *PTCA* as a function of molar ratio  $n_{Ru(III)}/n_{PTCA}$ .



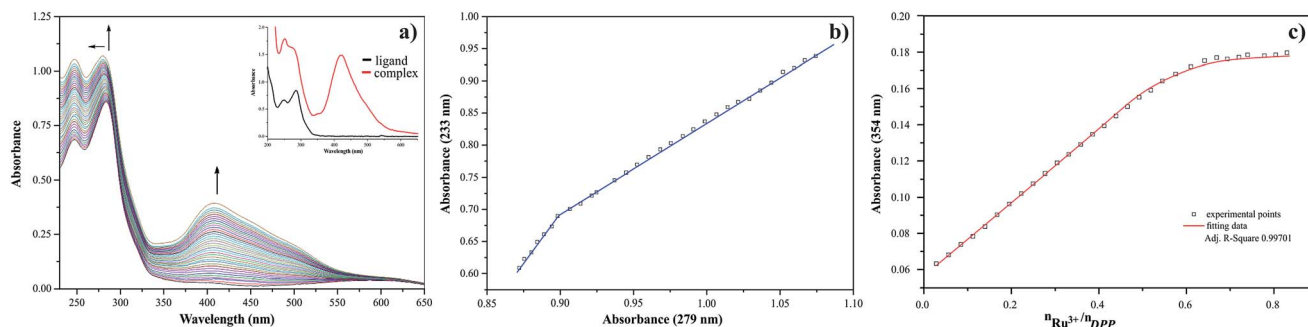


Fig. 6 (a) Spectrophotometric titration curves of 2,3-bis(2-pyridyl)pyrazine ( $5.15 \times 10^{-5}$  mol L<sup>-1</sup>) using a mixture of DPP at the same concentration and RuCl<sub>3</sub> ( $9.29 \times 10^{-4}$  mol L<sup>-1</sup>). (b) The A-diagram for Ru(III) ion with 2,3-bis(2-pyridyl)pyrazine for complexation process, major stoichiometry 1 : 2. (c) Dependence of absorbance at 354 nm for DPP as a function of molar ratio  $n_{Ru(III)}/n_{DPP}$ .

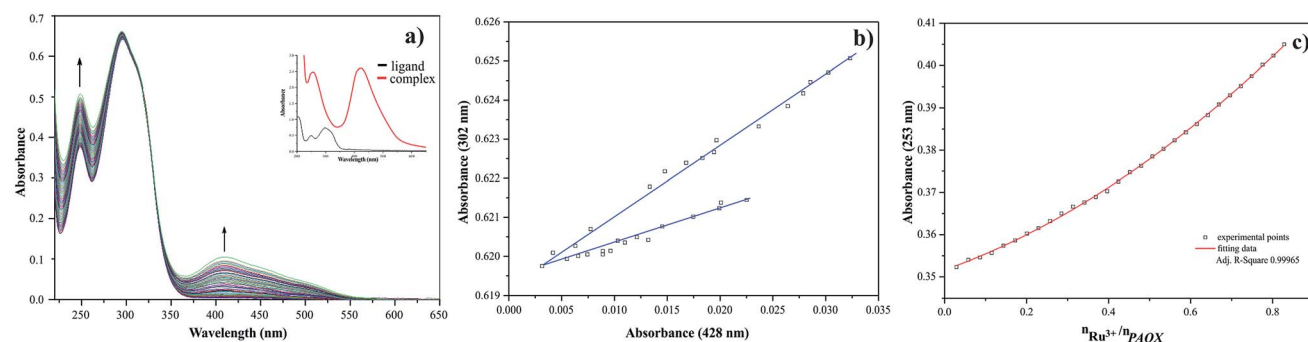


Fig. 7 (a) Spectrophotometric titration curves of pyrazine-2-amidoxime ( $1.70 \times 10^{-4}$  mol L<sup>-1</sup>) using a mixture of PAOX at the same concentration and RuCl<sub>3</sub> ( $2.76 \times 10^{-3}$  mol L<sup>-1</sup>). (b) The A-diagram for Ru(III) ion with pyrazine-2-amidoxime for complexation process, major stoichiometry 1 : 2. (c) Dependence of absorbance at 253 nm for PAOX as a function of molar ratio  $n_{Ru(III)}/n_{PAOX}$ .

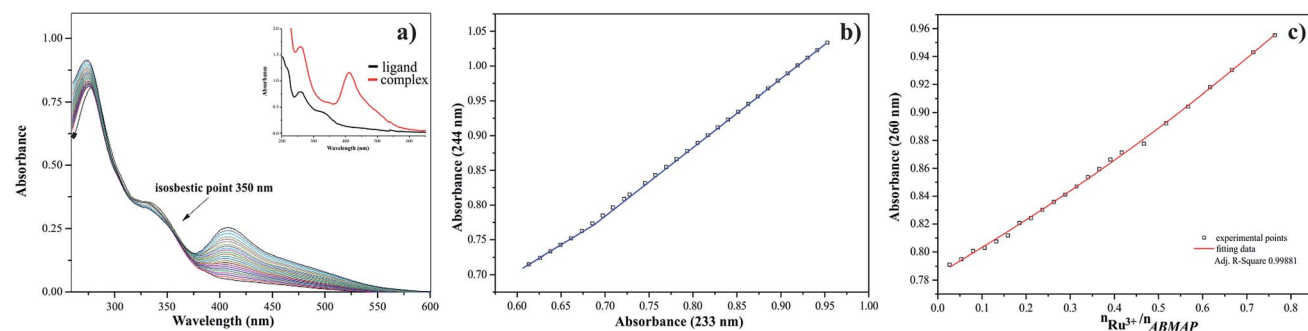


Fig. 8 (a) Spectrophotometric titration curves of 2-amine-5-bromo(3-methylamino)pyrazine ( $5.01 \times 10^{-5}$  mol L<sup>-1</sup>) using a mixture of ABMAP at the same concentration and RuCl<sub>3</sub> ( $1.00 \times 10^{-3}$  mol L<sup>-1</sup>). (b) The A-diagram plot for Ru(III) ion with 2-amine-5-bromo(3-methylamino)pyrazine for complexation process, major stoichiometry 1 : 2. (c) Dependence of absorbance at 260 nm for ABMAP as a function of molar ratio  $n_{Ru(III)}/n_{ABMAP}$ .

quantity of equilibria present in the arrangement studied. Two straight sections in the dependence of the absorbance at 279 nm to the absorbance at 428 nm confirmed the existence of two equilibria during the chelation process (Fig. 7b). The major stoichiometry of complex formation is 1 : 2, which corresponds to 0.5 value of molar ratio (Fig. 7c).

The results of titration process for ruthenium(III)-2-amino-5-bromo-3-(methylamino)pyrazine arrangement in MeCN have been presented in Fig. 8a. The intensities of absorption bands

increase, indicating a small hypsochromic effect. At the same time the isosbestic point and new maximum of absorption appeared at 350 nm and 414 nm, respectively. The presented spectral changes are the results of interactions between the hard acid – Ru(III) ion and donor atoms of ligand. To define the accurate number of equilibria presented in the system studied, the A-diagrams were plotted. The dependence of the absorbance at 244 nm to the absorbance at 233 nm showed two straight sections (Fig. 8b), suggesting that two formation constants



could be determined in this case. These remarks confirmed the dependence of absorbance at 260 nm for *ABMAP* as a function of molar ratio  $n_{\text{Ru(III)}}/n_{\text{ABMAP}}$  (Fig. 8c). In the arrangement studied, the values of molar ratio equal 0.5 which is consistent with stoichiometry 1 : 2 of the complex formation.

The proposed complexing equilibria models correspond to the formation of two Ru(III) ion–ligand complex of stoichiometry of 1 : 1 and 1 : 2 (metal : ligand) (eqn (1) and (2)). Based on the results from spectrophotometric measurements the values of gradual and cumulative formation constants for Ru(III) complexes were determined (Table 7).

Analyzing the values of cumulative stability constants of complexes in acetonitrile, it can be noticed that the most stable complex with ruthenium(III) ion is formed by 2,3-bis(2-pyridyl) pyrazine, while the weakest connection is formed by pyrazine-2-thiocarboxamide. The octahedral coordination is occupied by one water molecule, chlorine atom and azomethine nitrogen and nitrogen of the oxime or amine group in the case of *PAOX* and *PTCA*, respectively. The proposed binding set of Ru(III) complex with 2,3-bis(2-pyridyl)pyrazine includes nitrogen of the azomethine group and pyridyl ring. In case of *ABMAP*, the central atom is coordinated by two nitrogen atoms of amine and methylamine groups, respectively. During complexation processes more energetically favorable five-membered rings are formed, which is consistent with indicated coordination sites.

The stability constant values of monosubstituted pyrazine derivatives complexes in MeCN (*PAOX* and *PTCA*) increase with the number of donor atoms introduced to the substituents in the second position. Furthermore, the same trend can be observed when the increased number of substituents are introduced to the pyrazine ring (*ABMAP* and *DPP*). Disubstituted pyrazine derivatives have higher stability constants, which suggests that there occurs the establishment of coordination center consisting of two electron donating groups. Ruthenium(III) ion can bind to chelating elements of pyrazine derivatives, which is demonstrated in the  $\log K_1$  values. Lower  $\log K_2$  values (lower than  $\log K_1$ ) resulted from the binding second pyrazine derivative to the Ru(III) ion, decreasing the number of unoccupied places in the coordination sphere of the central atom.

Our experimental stability studies in aqueous solutions prove that one stability constant can be determined for

$[\text{Ru}(\text{ABMAP})(\text{OH}_2)_4]\text{Cl}_3$  and two for the other complexes. The existence of only one equilibrium in the case of  $[\text{Ru}(\text{ABMAP})(\text{OH}_2)_4]\text{Cl}_3$  is probably caused by both steric and electroinductive effects. Bromide anion is the biggest and most negative substituent in the pyrazine ring among the derivatives studied in this work.

### Biological assay – microbiological studies

The presented study was performed to estimate the influence of  $\text{RuCl}_3 \cdot 1.5\text{H}_2\text{O}$  and pure ligands (*PAOX*, *PTCA*, *DPP* and *ABMAP*) on growth and multiplication of selected bacterial strains and *Candida*. MIC and MBC tests were used to compare antibacterial and antifungal activity of Ru(III) complexes and 2 commercial antibiotics – Ciprofloxacin (for bacteria) and Fluconazole (for *Candida*). The presented results indicated that  $\text{RuCl}_3 \cdot 1.5\text{H}_2\text{O}$ , pure ligands (*PAOX*, *PTCA*, *DPP*, *ABMAP*) and Ru(III) complexes in a concentration from 2 to 200  $\mu\text{g mL}^{-1}$  (Table 8) have no antimicrobial activity.

In this case, only the  $[\text{RuCl}(\text{PAOX})_2(\text{OH}_2)]\text{Cl}_2$  complex exhibited low activity against tested Gram (–) bacteria in higher concentrations (MIC = 100  $\mu\text{g mL}^{-1}$ ) and Gram (+) bacteria: *E. faecalis* (MIC = 40  $\mu\text{g mL}^{-1}$ ) and *S. aureus* (MIC = 100  $\mu\text{g mL}^{-1}$ ). The  $[\text{RuCl}(\text{PAOX})_2(\text{OH}_2)]\text{Cl}_2$  complex tested against *C. albicans* presented strong antifungal activity (Table 9), *i.e.* at the level of 5  $\mu\text{g mL}^{-1}$ , which was similar to Fluconazole. Although the MIC of  $[\text{RuCl}(\text{PAOX})_2(\text{OH}_2)]\text{Cl}_2$  for the ATCC 90028 strain was 75  $\mu\text{g mL}^{-1}$ , combining this Ru complex with Fluconazole results in their synergistic antifungal activity. Combination of 4.7  $\mu\text{g mL}^{-1}$   $[\text{RuCl}(\text{PAOX})_2(\text{OH}_2)]\text{Cl}_2$  and 0.62  $\mu\text{g mL}^{-1}$  Fluconazole inhibited the growth of *C. albicans* (data not shown). Antifungal activity of  $[\text{RuCl}(\text{PAOX})_2(\text{OH}_2)]\text{Cl}_2$  complex may be caused by structural and steric similarity to ‘Ruthenium Red’ impurities like  $[\text{X}(\text{NH}_3)_4\text{Ru(III)}\text{ORu(IV)}(\text{NH}_3)_4\text{X}]^{3+}$  (where X =  $\text{OH}^-$ ,  $\text{Cl}^-$ ) that are known to block  $\text{Ca}^{2+}$  uptake in mitochondria blocking the cell respiration process.<sup>77</sup> The chelation of the  $\text{Ru}^{3+}$  ion by a Schiff base reduces its polarity and enables the complex to pass the phospholipid cell membrane because of the partial shift in Ru charge.<sup>78</sup>

The salt ( $\text{RuCl}_3 \cdot 1.5\text{H}_2\text{O}$ ), ligands (*PAOX*, *PTCA*, *DPP*, *ABMAP*) and other Ru(III) complexes presented low antifungal activity (MIC > 200  $\mu\text{g mL}^{-1}$ , data not shown). The yeast *C. albicans* is by

**Table 7** Values of parameters describing stabilities of Ru(III) complexes with pyrazine derivatives formed in MeCN and water during experiment. All results were determined at 25 °C

Complex cation	Molar ratio	Spectrophotometric technique					
		MeCN			H <sub>2</sub> O		
		$\log K_1$	$\log K_2$	$\log \beta$	$\log K_1$	$\log K_2$	$\log \beta$
$[\text{Ru}(\text{PAOX})_2(\text{OH}_2)_2]^{3+}$	1 : 2	4.55 ( $\pm 0.05$ )	4.49 ( $\pm 0.06$ )	9.04	3.61 ( $\pm 0.07$ )	7.15 ( $\pm 0.12$ )	10.76
$[\text{Ru}(\text{DPP})_2(\text{OH}_2)_2]^{3+}$	1 : 2	6.80 ( $\pm 0.02$ )	3.97 ( $\pm 0.02$ )	10.77	5.17 ( $\pm 0.16$ )	6.46 ( $\pm 0.19$ )	11.63
$[\text{Ru}(\text{PTCA})_2(\text{OH}_2)_2]^{3+}$	1 : 2	4.54 ( $\pm 0.02$ )	4.44 ( $\pm 0.03$ )	8.98	4.79 ( $\pm 0.11$ )	8.54 ( $\pm 0.17$ )	13.33
$[\text{Ru}(\text{ABMAP})_2(\text{OH}_2)_2]^{3+}$	1 : 2	4.84 ( $\pm 0.01$ )	4.64 ( $\pm 0.03$ )	9.48	4.65 ( $\pm 0.13$ )	— <sup>a</sup>	4.65

<sup>a</sup> Not found or undeterminable.



**Table 8** Comparison of minimal inhibitory concentrations (MIC) and minimal bactericidal concentrations (MBC) of salt, ligands (*PAOX*, *PTCA*, *DPP*, *ABMAP*), Ru(III) complexes and ciprofloxacin

Compound	Bacteria G (+)				Bacteria G (-)			
	<i>Enterococcus faecalis</i>		<i>Staphylococcus aureus</i>		<i>Klebsiella pneumoniae</i>		<i>Pseudomonas aeruginosa</i>	
	MIC	MBC	MIC	MBC	MIC	MBC	MIC	MBC
	$\mu\text{g mL}^{-1}$							
RuCl <sub>3</sub> ·1.5H <sub>2</sub> O	>200	>200	>200	>200	>200	>200	>200	>200
<i>PAOX</i>	>200	>200	>200	>200	>200	>200	>200	>200
<i>PTCA</i>	>200	>200	>200	>200	>200	>200	>200	>200
<i>DPP</i>	>200	>200	>200	>200	>200	>200	>200	>200
<i>ABMAP</i>	>200	>200	>200	>200	>200	>200	>200	>200
[RuCl( <i>PAOX</i> ) <sub>2</sub> (OH <sub>2</sub> )Cl] <sub>2</sub>	40	>200	100	>200	100	>200	100	>200
[RuCl( <i>PTCA</i> ) <sub>2</sub> (OH <sub>2</sub> )Cl] <sub>2</sub>	100	>200	>200	>200	>200	>200	150	>200
[RuCl <sub>2</sub> ( <i>ABMAP</i> ) <sub>2</sub> Cl]	100	>200	>200	>200	>200	>200	150	>200
[RuCl( <i>DPP</i> )(OH <sub>2</sub> ) <sub>3</sub> Cl] <sub>2</sub>	100	>200	>200	>200	>200	>200	150	>200
Ciprofloxacin	0.5	2	16	>256	<0.06	<0.06	1	2

**Table 9** Comparison of minimum inhibitory concentrations (MIC) of Ru(III) complex and Fluconazole

Compound	<i>Candida albicans</i>		
	ATCC 14053	ATCC 90028	ATCC 10231
	Minimum inhibitory concentration MIC ( $\mu\text{g mL}^{-1}$ )		
[RuCl( <i>PAOX</i> ) <sub>2</sub> (OH <sub>2</sub> )Cl] <sub>2</sub>	10	75	5
Fluconazole	5	2.5	5

far the most common human pathogenic *Candida* species and can cause a broad spectrum of diseases including skin, mucosal and systemic infections (candidiasis).<sup>79</sup> The antifungal agents available to treat fungal infections are limited. The clinical usefulness of drugs is hampered by their safety (undesirable side effects on patients are often associated with antifungal drugs).<sup>80</sup> Therefore, the development of new antifungal drugs is critical to continued effective therapy.

### Biological assay – cytotoxicity studies

The cytotoxicity of the [RuCl(*PAOX*)<sub>2</sub>(OH<sub>2</sub>)Cl]<sub>2</sub> complex as well as RuCl<sub>3</sub>·1.5H<sub>2</sub>O and *PAOX* was investigated using 3-(4,5-dimethylthiazol-2-yl)-2,5-diphenyltetrazolium bromide (MTT) cell viability assay that produce coloured formazan in the presence of living cells. The results obtained from this assay are as follows.

The cytotoxicity of the three tested compounds in bovine primary fibroblasts was assessed (Fig. 9a). RuCl<sub>3</sub>·1.5H<sub>2</sub>O caused about 15% loss of cell viability in concentration of 100  $\mu\text{g mL}^{-1}$ . *PAOX* seems to stimulate cell proliferation in concentrations range 40–100  $\mu\text{g mL}^{-1}$  but it appears to have a dose-dependent toxic effect at the higher concentrations (125  $\mu\text{g mL}^{-1}$  and 150  $\mu\text{g mL}^{-1}$ ) with a significant loss of approximately 30% cell

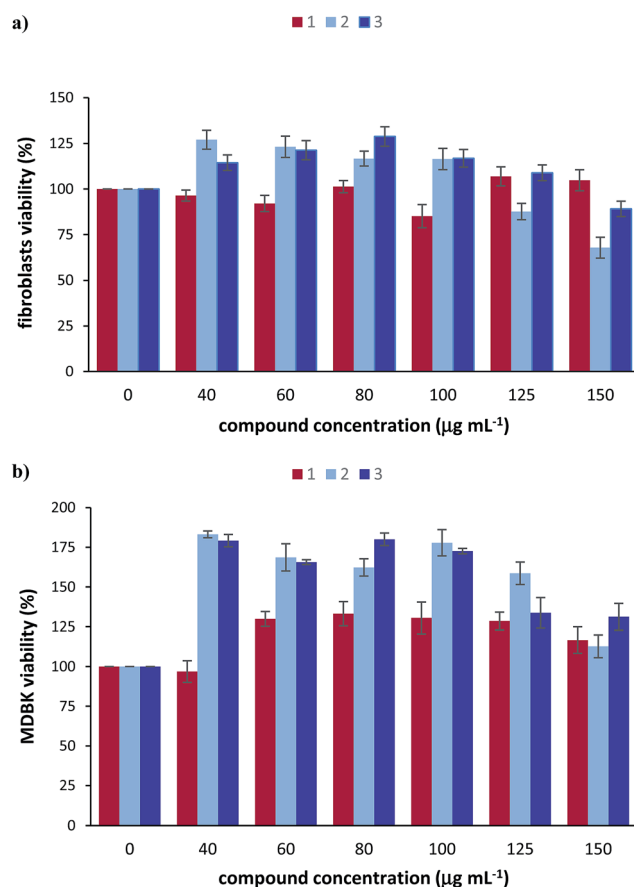


**Fig. 9** Percentage cell viability of the (a) bovine primary fibroblasts and (b) bovine MDBK cells derived from the MTT assay measurements after 24 h exposure of the cells to investigated compounds (1 – RuCl<sub>3</sub>·1.5H<sub>2</sub>O; 2 – *PAOX*; 3 – [RuCl(*PAOX*)<sub>2</sub>(OH<sub>2</sub>)Cl]<sub>2</sub>) of varying concentrations. The results shown are relative to the response of the control cells (treated with DMSO only) and they represent mean  $\pm$  standard deviation of three repeated experiments.



viability when the compound was introduced to the cells for 24 hours.  $[\text{RuCl}(\text{PAOX})_2(\text{OH}_2)]\text{Cl}_2$  complex caused slight cytotoxic effect (approximately 10%) only at the highest tested concentration of  $150 \mu\text{g mL}^{-1}$ . Data collected from the cell viability assay of the bovine MDBK cells show that none of the three tested compounds cause a cytotoxic effect, even in very high doses (Fig. 9b). What is more, it is evident that the cell viability in the presence of  $[\text{RuCl}(\text{PAOX})_2(\text{OH}_2)]\text{Cl}_2$  is over 100% after 24 h, indicating that it has proliferative effect on the tested cells.

### Biological assay – erythrocyte binding assay

To minimize interference from haemolysis, the spectra were analysed between 240 and 400 nm. For  $[\text{RuCl}(\text{PAOX})_2(\text{OH}_2)]\text{Cl}_2$  the best linearity in the investigated range was found to be at 282 nm ( $R^2 = 0.9965$ ). The concentration of  $[\text{RuCl}(\text{PAOX})_2(\text{OH}_2)]\text{Cl}_2$  in samples was determined with the use of the aforementioned wavelength. The obtained data suggest that the binding of  $[\text{RuCl}(\text{PAOX})_2(\text{OH}_2)]\text{Cl}_2$  to erythrocytes is a concentration dependant in an exponential manner. The obtained binding equation was  $y = 6.25 \times 10^{0.0184x}$  ( $R^2 = 0.9662$ ).

Based on the obtained data it can be determined that low concentrations ( $10 \mu\text{g mL}^{-1}$ ) do show significant binding to erythrocytes. After transmission through the cell membrane,  $\text{Ru}^{3+}$  ion could be reduced to  $\text{Ru}^{2+}$  ion that could compete for  $\text{Fe}^{2+}$  position in HEM.  $[\text{RuCl}(\text{PAOX})_2(\text{OH}_2)]\text{Cl}_2$  complex was deemed effective against fungi in lower ranges than those that show strong binding to erythrocytes.

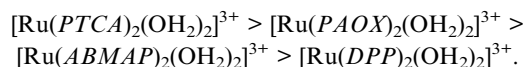
## Conclusions

The choice of the pyrazine derivative ligands for the present investigation was based on the consideration that the  $\text{Ru}(\text{III})$  ion (relatively hard Lewis acid) had high affinity for hard donor atom (O, N) groups in order to form stable complexes. From the analytical data and the physical studies discussed above, the selected pyrazine derivatives showed bidentate (bis-chelating) coordination mode. The synthesis of  $\text{Ru}(\text{III})$  with *PTCA*, *PAOX*, *DPP* and *ABMAP* has already been described in this paper. The binding set of three compounds included azomethine nitrogen and amine nitrogen. The central atom is a coordinated nitrogen atom of the azomethine group and pyridyl ring in  $[\text{RuCl}(\text{DPP})(\text{OH}_2)_3]\text{Cl}$ . The coordination number of the  $\text{Ru}(\text{III})$  complexes was 6, and on the basis of this coordination number, the structures proposed for the complexes were shown in Fig. 4. The geometries of the obtained complexes were found octahedral, which was consistent with the results of spectroscopic investigations. The  $^1\text{H}$  NMR and ESI-MS results complemented presented characterization of the  $\text{Ru}(\text{III})$  complexes as having octahedral species with a selected, bidentate pyrazine derivatives as ligand. The obtained analytical data were consistent with the proposed formula. The results of semi-empirical calculations showed that each  $\text{Ru}(\text{III})$  complex with selected pyrazine derivative had octahedral geometry, which was in conformity with the data obtained from spectroscopic and analytical experiments. X-ray crystallographic investigations, which might confirm the proposed structures, could not be

carried out as we failed to grow suitable crystals of any of these complexes.

The present study showed that coordination by the nitrogen donor atoms (amine, amide, and other nitrogen-containing groups) in the bidentate ligands could successfully stabilize the higher oxidation states of a transition metal. This was manifested in the stabilization of trivalent state of ruthenium in the  $[\text{RuCl}(\text{PAOX})_2(\text{OH}_2)]\text{Cl}_2$ ,  $[\text{RuCl}(\text{DPP})(\text{OH}_2)_3]\text{Cl}_2$ ,  $[\text{RuCl}(\text{PTCA})_2(\text{OH}_2)]\text{Cl}_2$ , and  $[\text{RuCl}_2(\text{ABMAP})_2]\text{Cl}$  complexes. The electrochemically generated one-electron oxidized and reduced species, *viz.*  $[\text{Ru}^{\text{IV}}\text{Cl}(\text{L})_n]$  and  $[\text{Ru}^{\text{II}}\text{Cl}(\text{L})_n]$  (where L denotes *PTCA* and *DPP* inside complexes) appeared to have a potential to serve as mild oxidants and reductants, respectively, and such possibilities are currently under study.

The presence of slight bathochromic and hypsochromic shifts combined with hyperchromic effect confirmed the interaction of metal ion with ligand. Spectrophotometric titrations results showed the presence of two  $\text{Ru}(\text{III})$  ion–ligand complexes of metal–ligand stoichiometry equal 1 : 1, and 1 : 2. The results obtained from experimental measurements enabled us to conclude that the complexes of ruthenium(III) examined in this work were found stable both in the solid state and solution, which was confirmed by the values of gradual and cumulative stability constants. They can be ordered in accord with their increasing stability:



In this rank  $\text{Ru}(\text{III})$  forms a complex of the highest stability with 2,3-bis(2-pyridyl)pyrazine, while with pyrazine-2-thiocarboxamide – the weakest one.

Among the coordination compounds of  $\text{Ru}(\text{III})$  only the complex  $[\text{RuCl}(\text{PAOX})_2(\text{OH}_2)]\text{Cl}_2$  presented strong antifungal activity. The complex causes no adverse health effects and may be used as a potential antifungal agent.

## Experiment protocols

### Material and methods

All chemicals of analytical purity grade were purchased from Sigma-Aldrich Co. Ltd.: pyrazine-2-amidoxime (pure 97%), pyrazine-2-thiocarboxamide (pure 97%), 2,3-bis(2-pyridyl)pyrazine (pure 98%), 2-amino-5-bromo-3-(methylamino)pyrazine (pure 97%), ruthenium(III) chloride hydrate (pure 99,98%). All reagents were used without further purification. The solutions were prepared with Hydrolab-Reference-purified water. The percentage compositions of the elements (C, H, N, S) of the synthesized compounds were determined using an element analyzer Carlo Erba EA 1108 CHNS. Infrared spectra of  $\text{Ru}(\text{III})$  complexes were recorded as potassium bromide (KBr) pellets using Bruker Infrared Spectrometer in the range of  $4000\text{--}400 \text{ cm}^{-1}$ . The  $^1\text{H}$  NMR spectra of  $\text{Ru}(\text{III})$  complexes were recorded on a Bruker AVANCE III 500 MHz instrument in  $\text{DMSO-d}_6$ . The chemical shifts values were reported in ppm ( $\delta$ ) and were applied indirectly to tetramethylsilane as a signal of solvent



(2.49 for  $^1\text{H}$  in  $\text{DMSO-d}_6$ ). ESI-MS spectra of  $\text{Ru(III)}$  complexes were recorded in positive ion mode by direct injection at a  $5 \mu\text{L min}^{-1}$  flow rate using a Bruker Daltonics HCT Ultra high-resolution mass spectrometer equipped with conventional ESI source. All measurements were performed at room temperature.

The electronic absorption spectra were recorded in MeCN on a Perkin Elmer Lambda 650 spectrophotometer in the range of 250–700 nm with a spectral band width of 2 nm. The determination of the composition and stabilities of the examined ruthenium(III) complexes were performed with the spectrophotometric titration method in the range of 200–600 nm. The solutions of the studied pyrazine derivatives and metal  $\text{Ru(III)}$  cation were prepared directly before measurements and were maintained at a constant temperature of  $25^\circ\text{C}$ . The spectrophotometric titrations were carried out at a constant ligand concentration. The concentration of metal ion was about 20 times higher than ligand. Conductivity measurements were obtained using an ELMETRON CC-401 conductivity meter, at  $25^\circ\text{C}$  in water as a solvent, using concentrations of  $10^{-3} \text{ mol} \cdot \text{dm}^{-3}$  for all synthesized complexes. Thermal decompositions were measured by means of a thermal equalizer TG209 Netzsch. All experiments were carried out in argon atmosphere. The analyzer was equipped with a programmed temperature controller, which automatically maintains constant temperature during thermal events. The TG weight loss was measured from 20 to  $850^\circ\text{C}$  at a heating rate of  $15^\circ\text{C min}^{-1}$ . Infrared spectra were registered in Nujol mulls using a Bruker IFS 66 spectrophotometer. All the measurements were verified at least twice.

### Synthesis of the complexes

Ruthenium(III) chloride hydrate (0.41 g; 1.75 mmol), lithium chloride (4.19 g; 100.00 mmol) and 0.49 g (3.52 mmol) pyrazine-2-thiocarboxamide (0.48 g – 3.47 mmol of pyrazine-2-amidoxime) were dissolved in 50 mL dimethylformamide. The mixture was heated at reflux for 8 h and stirred magnetically throughout this period. After the solution was cooled down to room temperature, 250 mL acetone was added and the resulting solution was cooled in a fridge (at  $0^\circ\text{C}$ ) overnight. Filtering yielded a red-black solution and a dark brown microcrystalline product for *PTCA* and a blue-black solution and a dark navy blue microcrystalline product for *PAOX*. The precipitate was washed three times with 25 mL portions of diethyl ether and then left to slow evaporation at room temperature. In a similar way – with the use of 0.29 g (1.24 mmol) ruthenium(III) chloride hydrate, lithium chloride (4.19 g; 100.00 mmol) and 0.59 g (2.52 mmol) *DPP* (0.51 g; 2.52 mmol) *ABMAP* – the black powder of  $[\text{RuCl}(\text{DPP})(\text{OH}_2)_3]\text{Cl}_2$  complex and the black-green powder of  $[\text{RuCl}_2(\text{ABMAP})_2]\text{Cl}$  were collected after a few days. Their solubilities in water, acetonitrile and DMSO were confirmed for all synthesized complexes.

### Electrochemical study

All cyclic voltammetry (CV) experiments were performed under inert gas atmosphere. Voltammetric recordings were made

using a Gamry Instruments 600 electrochemical analyzer. A platinum-bead working, platinum-coil counter electrode and saturated calomel reference electrode (SCE) were used for CV measurements. Cyclic voltammograms were recorded under argon gas atmosphere in MeCN at room temperature. The concentration of the complexes was 1 mM in the electrolyte solution, where commercially obtained  $[\text{n}-(\text{C}_4\text{H}_9)_4\text{N}]\text{ClO}_4$  (TBAP) was used as a supporting electrolyte. The voltage scan rate during the CV measurements was  $100 \text{ mV s}^{-1}$ . Controlled potential electrolysis at the anodic peak potential was carried out with an Ag-wire reference electrode after making a correction between the SCE and the Ag-wire (280 mV for SCE).

### Molecular modeling

Geometry optimization has been performed with the use of semi-empirical PM3 and AM1 methods<sup>81</sup> using the Hyperchem 8.<sup>82</sup> The correct stereochemistry was assured through the manipulation and modification of the molecular coordinates to obtain reasonable low energy molecular geometries at AM1 and PM3, (Polak-Ribiere) RMS 0.01 kcal.

### Antimicrobial and antifungal activity

We studied the antimicrobial and antifungal activity of  $\text{Ru(III)}$  complexes with *PAOX*, *PTCA*, *DPP*, *ABMAP* and pure ligands (*PAOX*, *PTCA*, *DPP*, *ABMAP*) and the metal salt  $\text{RuCl}_3 \cdot 1.5\text{H}_2\text{O}$  within wide concentration ranges ( $2.5\text{--}200 \mu\text{g mL}^{-1}$ ).

We used the following strains either resistant or susceptible to antibiotics from 4 species of human bacterial pathogens (hospital isolates obtained from the Laboratory of Microbiology of the Provincial Hospital in Gdansk, Poland are stored in the Faculty of Biotechnology, UG & MUG, Poland): *Enterococcus faecalis* G (+), *Staphylococcus aureus* G (+), *Klebsiella pneumoniae* G (–) and *Pseudomonas aeruginosa* G (–). The isolates were tested for resistance to 12 antibiotics from the classes of:  $\beta$ -lactams, aminoglycosides, glycopeptides macrolide, fluoroquinolone and lincosamide.<sup>83</sup> We also tested 3 strains of *Candida albicans* (ATCC 14053, ATCC 90028 and ATCC 10231) susceptible to Fluconazole (ThermoFisher, Germany). The bacteria and fungi were grown on BHI medium (BTL, Poland) at  $37^\circ\text{C}$ . The minimum bactericidal concentrations (MBC) of the tested compounds required to achieve the desired antimicrobial effect in planktonic culture were determined using the method described previously.<sup>84</sup> For fungi the minimum inhibitory concentration (MIC) was determined using the broth microdilution method according to CLSI method with the inoculum of  $2.5 \times 10^3 \text{ CFU mL}^{-1}$ . Additional tests were performed for *Candida*, involving microdilution broth checkerboard techniques *in vitro* which established pharmacodynamic interactions between  $[\text{RuCl}(\text{PAOX})_2(\text{OH}_2)]\text{Cl}_2$  and the antibiotic Fluconazole, according to the method described by Meletiadis *et al.*<sup>85</sup>

### Cell culture and treatment with compounds

Primary bovine fibroblasts isolated from calves' ear was cultured in a complete cell culture medium, consisting of DMEM (Dulbecco's Modified Eagle Medium, Sigma)



supplemented with 15% heat-inactivated fetal bovine serum (FBS, Gibco), 2 mM L-glutamine (Invitrogen) and 10 mL L<sup>-1</sup> of Antibiotic Antimycotic Solution (Sigma), at 37 °C in a 5% CO<sub>2</sub> humidified atmosphere. Madin-Darby bovine kidney (MDBK) cells (American Type Culture Collection, ATCC) were maintained at the same conditions in RPMI-1640 medium (Roswell Park Memorial Institute, Sigma) supplemented with 8% heat-inactivated fetal bovine serum, 2 mM L-glutamine and 10 mL L<sup>-1</sup> of Antibiotic Antimycotic Solution (Sigma). Stock solutions of investigated compounds (10 mg mL<sup>-1</sup>) were prepared in dimethyl sulfoxide (DMSO, PanReac AppliChem). Prior to the introduction of tested compounds, 100 μL per well of cells with a cell density of 7.5 × 10<sup>3</sup> cells per well were seeded in 96-well plates for 24 h. Then the medium was removed and 100 μL of the different concentrations of RuCl<sub>3</sub>·1.5H<sub>2</sub>O, PAOX or [RuCl(PAOX)<sub>2</sub>(OH<sub>2</sub>)Cl<sub>2</sub>] solutions prepared in complete medium from 10 mg mL<sup>-1</sup> stocks were added to the cells in each well and incubated for another 24 hours. The control consisted of only the cells and culture medium with the volume of DMSO equal to the volume of suspended compounds in their highest tested concentration.

### MTT assay

MTT stock solution (5 mg mL<sup>-1</sup>) was prepared in 1× PBS. Upon exposing the fibroblasts or MDBK cells to the investigated compounds suspensions for 24 h, the MTT solution (20 μL) was added to each well and incubated at 37 °C under 5% CO<sub>2</sub> for 3.5 hours. The MTT solution was removed and replaced with MTT solvent (150 μL) to dissolve the insoluble purple formazan crystals produced by the living cells. The plates were covered with tinfoil and gently agitated on an orbital shaker for 15 min, after which they were placed on a plate reader to measure the absorbance at 570 nm. The effects of the tested compounds cell viability were calculated using cells treated with DMSO as control (set as 100%). All experiments were repeated three times.

### Erythrocyte binding assay

A 2% solution of 100% sheep red blood cells (BioCity Nottingham, United Kingdom) in physiological salt (0.9% NaCl) was freshly prepared before use. The solution was spiked with [RuCl(PAOX)<sub>2</sub>(OH<sub>2</sub>)Cl<sub>2</sub>] to a final concentration in the range between 5 and 150 μg mL<sup>-1</sup>. Samples were incubated in 37 °C for 1 hour. After the incubation they were centrifuged at 10 000 RCF (relative centrifugal force) for 10 minutes. The supernatant was collected and analyzed using a Perkin Elmer Lambda 25 spectrophotometer in 200–700 nm range. The obtained spectra were used to determine the concentration of unbound [RuCl(PAOX)<sub>2</sub>(OH<sub>2</sub>)Cl<sub>2</sub>] in the supernatant. Seven point three level calibration curve for [RuCl(PAOX)<sub>2</sub>(OH<sub>2</sub>)Cl<sub>2</sub>] was performed prior to sample analysis. All experiments were repeated in triplicate.

## Acknowledgements

The authors gratefully acknowledge the financial support from the Polish Ministry of Science and Higher Education [grant

number BMN 538-8236-B698-15], [grant number BMN 538-8236-B663-15], [DS/530-8236-D601-15] and [DS/530-M035-D568-15]. The support of Prof. Zbigniew Kaczyński from the Laboratory of Structural Biochemistry at the Faculty of Chemistry University of Gdańsk in discussion of ESI-MS spectra is greatly appreciated.

## References

- 1 R. E. Morris, R. E. Aird, P. S. Murdoch, H. Chen, J. Cummings, N. D. Hughes, S. Parson, A. Parkin, G. Boyd, D. I. Jodrell and P. J. Sadler, *J. Med. Chem.*, 2001, **44**, 3616.
- 2 M. Galanski, V. B. Arion, M. A. Jakupec and B. K. Keppler, *Curr. Pharm. Des.*, 2003, **9**, 2078.
- 3 P. Pigeon, S. Top, A. Vessières, M. Huché, E. A. Hillard, E. Salomon and G. Jaouen, *J. Med. Chem.*, 2005, **48**, 2814.
- 4 X. Meng, M. L. Leyva, M. Jenny, I. Gross, S. Benosman, B. Fricker, S. Harlepp, P. Hébraud, A. Boos, P. Wlosik, P. Bischoff, C. Sirlin, M. Pfeffer, J. Loeffler and C. Gaidon, *Cancer Res.*, 2009, **69**, 5458.
- 5 V. Brabec and O. Nováková, *Drug Resist. Updates*, 2006, **9**(111), 1368.
- 6 C. S. Allardynce and P. J. Dyson, *Platinum Met. Rev.*, 2001, **45**, 62.
- 7 R. L. Williams, N. H. Toft, B. Winkel and K. J. Brewer, *Inorg. Chem.*, 2003, **42**, 4394.
- 8 A. Bergamo and G. Sava, *Dalton Trans.*, 2007, **13**, 1267.
- 9 C. G. Hartinger, M. A. Jakupec, S. Zorbas-Seifried, M. Groessl, A. Egger, W. Berger, H. Zorbas, P. J. Dyson and B. K. Keppler, *Chem. Biodiversity*, 2008, **5**, 2140.
- 10 C. G. Hartinger, S. Zorbas-Seifried, M. A. Jakupec, B. Kynast, H. Zorbas and B. K. Keppler, *J. Inorg. Chem.*, 2006, **100**, 891.
- 11 G. Sava, E. Alessio, A. Bergamo and G. Mestroni, *Top. Biol. Inorg. Chem.*, 1999, **1**, 143.
- 12 G. Sava, I. Capozzi, K. Clerici, G. Gagliardi, E. Alessio and G. Mestroni, *Clin. Exp. Metastasis*, 1998, **16**, 371.
- 13 A. Levina, A. Mitra and P. A. Lay, *Metallomics*, 2009, **1**, 458.
- 14 L. Trynda-Lemiesz, A. Karaczyn, B. K. Keppler and H. Kozłowski, *J. Inorg. Biochem.*, 2000, **78**, 341.
- 15 O. Mazuryk, K. Kurpiewska, K. Lewinski, G. Stochel and M. Brindell, *J. Inorg. Biochem.*, 2012, **116**, 11.
- 16 A. Calzolari, I. Oliviero, S. Deaglio, G. Mariani, M. Biffoni, N. M. Sposi, F. Malavasi, C. Peschle and U. Testa, *Blood Cells, Mol., Dis.*, 2007, **39**, 82.
- 17 S. Kapitza, M. A. Jakupec, M. Uhl, B. K. Keppler and B. Marian, *Cancer Lett.*, 2005, **226**, 115.
- 18 K. S. Smalley, R. Contractor, N. K. Haass, A. N. Kulp, G. E. Atilla-Gokcumen and D. S. Williams, *Cancer Res.*, 2007, **67**, 209.
- 19 W. H. Ang, A. Casini, G. Sava and P. J. Dyson, *J. Org. Chem.*, 2011, **696**, 989.
- 20 M. R. Kamal and R. Levine, *J. Org. Chem.*, 1962, **27**, 1360.
- 21 D. Pancechowska-Ksepko, H. Foks, M. Janowiec and Z. Zwolska-Kwiek, *Acta Pol. Pharm.*, 1988, **45**, 193.
- 22 W. Rudnicka, H. Foks, M. Janowiec and Z. Zwolska-Kwiek, *Acta Pol. Pharm.*, 1986, **43**, 523.



- 23 M. H. Cynamon and S. P. Klemens, *J. Med. Chem.*, 1992, **35**, 1212.
- 24 K. Gobis, H. Foks, A. Kędzia, M. Wierzchowska, E. Kwapisz, Z. Zwolska and E. Augustynowicz-Kopeć, *Acta Pol. Pharm.*, 2006, **63**, 39.
- 25 M. Dolezal, P. Cmedlova and L. Palek, *Eur. J. Med. Chem.*, 2008, **43**, 1105.
- 26 T. B. Adams, J. Doull and V. J. Ferron, *Food Chem. Toxicol.*, 2002, **40**, 429.
- 27 D. Frederic, M. Giulio, L. Didier, S. Therese, S. Y. Jacques, R. J. Francois and M. Jacqueline, *Eur. J. Med. Chem.*, 2010, **45**, 3564.
- 28 G. G. Dubinina, M. O. Platonov, S. M. Golovach, P. O. Borysko, A. O. Tolmachov and Y. M. Volovenko, *Eur. J. Med. Chem.*, 2006, **41**, 727.
- 29 M. Shailaja, A. Manjula, S. Venkateshwarlu, B. Vittal Rao and A. Anthony, *Eur. J. Med. Chem.*, 2010, **45**, 5208.
- 30 A. Saxena, J. K. Koacher and J. P. Tandon, *J. Antibact. Antifungal Agents*, 1981, **9**, 435.
- 31 F. Beckford, J. Thessing, J. Woods, J. Didion, N. Gerasimchuk, A. Gonzalez-Sarrias and N. P. Seeram, *Metallomics*, 2011, **3**, 491.
- 32 A. M. Pizarro, M. Melchart, A. Habtemariam, L. Salassa, F. P. A. Fabbiani, S. Parsons and P. J. Sadler, *Inorg. Chem.*, 2010, **49**, 3310.
- 33 W. Kandioller, C. G. Hartinger, A. A. Nazarov, C. Bartel, M. Skocic, M. A. Jakupec, V. B. Arion and B. K. Keppler, *Chem.-Eur. J.*, 2009, **15**, 12283.
- 34 M. J. M. Cambell, *Coord. Chem. Rev.*, 1975, **15**, 279.
- 35 D. R. Williams, *Chem. Rev.*, 1972, **72**, 102.
- 36 R. K. Agarwal and S. Prasad, *Turk. J. Chem.*, 2004, **28**, 691.
- 37 J. A. Streeky, D. G. Pillsburg and D. H. Busch, *Inorg. Chem.*, 1984, **19**, 3148.
- 38 V. Chinnusamy and K. Natarajan, *Synth. React. Inorg. Met.-Org. Chem.*, 1993, **23**, 889.
- 39 R. C. Saxena, C. L. Jain, R. Benjamin and S. K. Sangal, *J. Indian Chem. Soc.*, 1986, **63**, 435.
- 40 A. Chylewska, M. Ogryzek, R. Hałasa, A. Dąbrowska, L. Chmurzyński and M. Makowski, *J. Coord. Chem.*, 2014, **67**, 2885.
- 41 A. Chylewska, K. Turecka, A. Dąbrowska, W. Werel and L. Chmurzyński, *Int. J. Adv. Pharm., Biol. Chem.*, 2013, **2**, 454.
- 42 A. Chylewska, D. Jacewicz, D. Zarzeczańska and L. Chmurzyński, *J. Chem. Thermodyn.*, 2008, **40**, 1290.
- 43 A. Chylewska, M. Ogryzek, L. Chmurzyński and M. Makowski, *J. Coord. Chem.*, 2015, **68**, 3761.
- 44 A. Chylewska, A. Sikorski, M. Ogryzek and M. Makowski, *J. Mol. Struct.*, 2016, **1105**, 96.
- 45 S. C. Tripathi and S. Paul, Stability constants of Ru(III), Rh(III), Pd(III), Os(VIII), Ir(III) and Pt(IV) chelates with O-coumaric acid, *J. Inorg. Nucl. Chem.*, 1973, **35**, 2465–2470.
- 46 D. Chatterjee and A. Mitra, Ruthenium Polyaminocarboxylate Complexes. Prospects for their use as metallopharmaceuticals, *Platinum Met. Rev.*, 2006, **50**, 2–12.
- 47 M. Delferro, L. Marchio, M. Tegoni, S. Tardito, R. Franchi-Gazzola and M. Lanfranchi, Synthesis, structural characterisation and solution chemistry of ruthenium(III) triazole-thiadiazine complexes, *Dalton Trans.*, 2009, 3766–3773.
- 48 N. Ljubijankić, A. Zahirović, E. Turkušić and E. Kahrović, DNA Binding Properties of Two Ruthenium(III) Complexes Containing Schiff Bases Derived from Salicylaldehyde: Spectroscopic and Electrochemical Evidence of CT DNA Intercalation, *Croat. Chem. Acta*, 2013, **86**, 215–222.
- 49 D. Musumeci, L. Rozza, A. Merlino, L. Paduano, T. Marzo, L. Massai, L. Messori and D. Montesarchio, Interaction of anticancer Ru(III) complexes with single stranded and duplex DNA model systems, *Dalton Trans.*, 2015, **44**, 13914–13925.
- 50 R. K. Agarwal, *Pol. J. Chem.*, 1991, **65**, 1211.
- 51 R. K. Agarwal and S. Prasad, *Turk. J. Chem.*, 2005, **29**, 289.
- 52 A. Natarajan and S. Pragasam, *Asian J. Chem.*, 1995, **7**, 757.
- 53 A. H. Velders, B. van der Geest, H. Kooijman, A. L. Spek, J. G. Haasnoot and J. Reedijk, *Eur. J. Inorg. Chem.*, 2001, **2**, 369.
- 54 K. van der Schilden, A. H. Velders, J. G. Haasnoot and J. Reedijk, *J. Inorg. Biochem.*, 2001, **86**, 466.
- 55 H. Gunther, *NMR Spectroscopy*, John Wiley & Sons Ltd, 2001.
- 56 V. K. Sharma, A. Srivastava and S. Srivastava, *J. Serb. Chem. Soc.*, 2006, **71**, 917.
- 57 A. Garza-Ortiz, P. U. Maheswari, M. Siegler, A. L. Spek and J. Reedijk, *Inorg. Chem.*, 2008, **47**, 6964.
- 58 M. Delferro, L. Marchio, M. Tegoni, S. Tardito, R. Franchi-Gazzola and M. Lanfranchi, *Dalton Trans.*, 2009, **19**, 3766.
- 59 P. Dolezel and V. Kuban, *Chem. Pap.*, 2002, **56**, 236.
- 60 D. Musumeci, L. Rozza, A. Merlino, L. Paduano, T. Marzo, L. Massai, L. Messori and D. Montesarchio, *Dalton Trans.*, 2015, **44**, 13914.
- 61 S. A. Hofstadler and K. A. Sannes-Lowery, *Nat. Rev. Drug Discovery*, 2006, **5**, 585.
- 62 F. Lachaud, A. Quaranta, Y. Pellegrin, P. Dorlet, M. F. Charlot, S. Un, W. Leibl and A. Aukauloo, *Angew. Chem.*, 2005, **44**, 1536.
- 63 G. Venkatachalam, S. Matheswaran and R. Ramesh, *Indian J. Chem.*, 2005, **44**, 705.
- 64 V. K. Sharma, S. Srivastava and A. Srivastava, *Bioinorg. Chem. Appl.*, 2007, **2007**, 1.
- 65 C. K. Jorgensen, *Acta Chem. Scand.*, 1956, **10**, 518.
- 66 Y. Tanabe and S. Sugano, *J. Phys. Soc. Jpn.*, 1954, **9**, 753.
- 67 J. Wang, Y. Zhao, X. Jin, L. Yang and H. Wang, *Spectrochim. Acta, Part A*, 2014, **122**, 649.
- 68 R. Abu-Eittah and M. M. Hammed, *Bull. Chem. Soc. Jpn.*, 1984, **57**, 844.
- 69 S. Chandra, *Nano-Metal Chemistry*, 1992, **22**, 1565.
- 70 A. Z. El-Sonbati, A. A. El-Bindary, A. El-Dissouky, T. M. El-Gogary and A. S. Hilali, *Spectrochim. Acta, Part A*, 2002, **58**, 1623.
- 71 E. M. Jouad, A. Riou and M. Allain, *Polyhedron*, 2001, **20**, 67.
- 72 R. Ramesh and S. Maheswaran, *J. Inorg. Biochem.*, 2003, **96**, 457.
- 73 L. Mishra, R. Prajapati and K. K. Pandey, *Spectrochim. Acta, Part A*, 2008, **70**, 79.
- 74 G. P. Puthilibai, S. Vasudhevan, S. K. Rani and G. Rajagopal, *Spectrochim. Acta, Part A*, 2009, **72**, 796.



## Paper

- 75 J. Kostrowicki and A. Liwo, *Comput. Chem.*, 1987, **11**, 193.
- 76 D. A. Jose, D. K. Kumar, B. Ganguly and A. Das, *Org. Lett.*, 2004, **6**, 3445.
- 77 W. L. Ying, J. Emerson, M. J. Clarke and D. R. Sanadi, *Biochemistry*, 1991, **30**, 4949.
- 78 M. J. Clarke, *Coord. Chem. Rev.*, 2003, **236**, 209.
- 79 G. Moran, D. Coleman and D. Sullivan, in *Candida and Candidiasis*, ed. R. A. Calderone and C. J. Clancy, ASM Press, 2nd edn, 2012.
- 80 D. Gozalbo, P. Roig, E. Villamón and M. L. Gil, *Curr. Drug Targets: Infect. Disord.*, 2004, **4**, 117.
- 81 N. L. Allinger, *J. Am. Chem. Soc.*, 1977, **99**, 8127.
- 82 *HyperChem version 8.0*, Hypercube Inc., 2002.
- 83 K. Bogucka, A. Królicka, W. Kamysz, T. Ossowski, J. Łukasiak and E. Łojkowska, *Pol. J. Microbiol.*, 2004, **53**, 41.
- 84 M. Krychowiak, M. Grinholc, R. Banasiuk, M. Krauze-Baranowska, D. Glod, A. Kawiak and A. Królicka, *PLoS One*, 2014, **9**, e115727.
- 85 J. Meletiadis, S. Pournaras, E. Roilides and T. J. Walsh, *Antimicrob. Agents Chemother.*, 2010, **54**, 602.

